A direct link between abscisic acid sensing and the chromatin remodeling ATPase BRAHMA via core ABA signaling pathway components

Marta Peirats-Llobet*[1], Soon-Ki Han*[2], Miguel Gonzalez-Guzman[1], Cheol Woong Jeong[2], Lesia Rodriguez[1], Borja Belda-Palazon[1], Doris Wagner[†2] and Pedro L. Rodriguez[†1]

[1]Instituto de Biología Molecular y Celular de Plantas, Consejo Superior de Investigaciones Científicas-Universidad Politécnica de Valencia, 46022 Valencia, Spain

[2]Department of Biology, University of Pennsylvania, Philadelphia, Pennsylvania 19104

*Both authors contributed equally to this work

[†]Corresponding authors: Wagner, D. (wagnerdo@sas.upenn.edu) and Rodriguez, P.L. (prodriguez@ibmcp.upv.es)

Running title: An ABA phosphorylation switch regulates BRM

Key words: abscisic acid, hormone signaling, chromatin remodeling

ABSTRACT

Optimal response to drought is critical for plant survival and will impact biodiversity and crop performance during climate change. Mitotically heritable epigenetic or dynamic chromatin state changes have been implicated in the plant response to the drought stress hormone abscisic acid (ABA). The *Arabidopsis* SWI/SNF chromatin remodeling ATPase BRAHMA (BRM) modulates response to ABA by preventing premature activation of stress response pathways during germination. We show that core ABA signaling pathway components physically interact with BRM and posttranslationally modify BRM by phospho-/dephosphorylation. Genetic evidence suggests that BRM acts downstream of SnRK2.2/2.3 kinases and biochemical studies identified phosphorylation sites in the C-terminal region of BRM at SnRK2 target sites that are evolutionarily conserved. Finally, the phosphomimetic BRM$^{S1760D\ S1762D}$ mutant displays ABA hypersensitivity. Prior studies showed that BRM resides at target loci in the ABA pathway in the presence and absence of the stimulus, but is only active in the absence of ABA. Our data suggest that SnRK2-dependent phosphorylation of BRM leads to its inhibition and PP2CA-mediated dephosphorylation of BRM restores ability of BRM to repress ABA response. The findings point to the presence of a rapid phosphorylation-based switch to control BRM activity; this property could be potentially harnessed to improve drought tolerance in plants.

INTRODUCTION

The stress hormone abscisic acid (ABA) elicits plant responses through binding to soluble PYRABACTIN RESISTANCE1 (PYR1)/PYR1-LIKE (PYL)/REGULATORY COMPONENTS OF ABA RECEPTORS (RCAR) receptors, which constitute a 14-member family in *Arabidopsis thaliana*. PYR/PYL/RCAR receptors perceive ABA in different subcellular locations (Rodriguez et al., 2014) and as a result, form ternary complexes with clade A protein phosphatases type 2C (PP2Cs), thereby inactivating these negative regulators of ABA signaling (Ma et al., 2009; Park et al., 2009; Santiago et al., 2009; Nishimura et al., 2010). Therefore, ABA sensing prevents the PP2C-mediated dephosphorylation of ABA-activated sucrose non-fermenting 1-related protein kinases (SnRKs) subfamily 2 (SnRK2s), i.e. SnRK2.2/D, 2.3/I and 2.6/E/OST1, and ABA receptors indirectly control the activity of these SnRK2s by allowing cis- and trans-autophosphorylation of the SnRK2 activation loop (Cutler et al., 2010; Soon et al., 2012; Ng et al., 2012; Minkoff et al., 2015). It results in the activation of a SnRK2-dependent phosphorylation cascade affecting a high number of targets in the plant cell (Wang et al., 2013; Umezawa et al., 2013). As a result, ABA-activated SnRK2s regulate different cellular processes, among them ion transport, cytosolic pH and transcriptional response to ABA (Planes et al., 2015; Yoshida et al., 2015). Conversely, in the absence of ABA SnRK2 kinases are kept in an inactive state by clade A PP2Cs (Vlad et al., 2009; Umezawa et al., 2009).

ABA signaling regulates plant growth and development as well as stress responses (Cutler et al., 2010; Finkelstein et al., 2013). Plant developmental processes regulated by ABA are embryo maturation, seed development, dormancy and germination, seedling establishment, primary and lateral root growth and transition from vegetative to reproductive stage (Cutler et al., 2010; Finkelstein et al., 2013). In addition ABA mediates response to both biotic and abiotic stresses (Cutler et al., 2010; Finkelstein et al., 2013). ABA signaling, in addition to key effects on ion transporters at the plasma membrane, leads to coordinated transcriptional reprogramming of gene expression in a ligand-dependent manner (Cutler et al., 2010; Finkelstein et al., 2013). Inducible alteration of gene expression requires changes in the chromatin state (Weake

and Workmann 2010). Chromatin-mediated control of gene expression involves enzymes that covalently modify histones (e.g. by acetylation, methylation, phosphorylation and ubiquitylation) or the DNA (methylation) as well as non-covalent change nucleosome occupancy or positioning through chromatin remodeling complexes (CRCs), such as SWI/SNF subgroup complexes that form around BRAHMA (BRM) (Han et al., 2015). Indeed, ABA response has been linked to mitotically heritable and dynamic chromatin state changes (Chinnusamy and Zhu, 2009; Yaish et al. 2011, Han et al, 2014). For example, chromatin remodeling (Han et al., 2012), histone deacetylation (Zhu et al., 2008; Luo et al., 2012; Ryu et al., 2014), and histone demethylation (Zhao et al., 2015) have been reported to regulate ABA response.

Specifically, with respect to chromatin remodeling, loss- or reduction-of-function of the SWI/SNF ATPase *BRM* or associated complex component *SWI3C* causes ABA-hypersensitivity during post-germination growth due to de-repression of a positive regulator of ABA response, the bZIP transcription factor *ABA INSENSITIVE 5* (*ABI5*) (Han et al., 2012). While basal levels of *ABI5* were increased in *brm* mutants, fold induction of *ABI5* in ABA versus mock treated plants was similar in the *brm* mutant as in the wild type plants, suggesting that BRM is specifically required to prevent *ABI5* expression in the absence of the cue. Accordingly, BRM maintains a well positioned nucleosome at the *ABI5* transcription start site in the absence of ABA and this nucleosome is destabilized upon ABA sensing (Han et al., 2012). Intriguingly, BRM binds to the critical region at this locus in the absence and in the presence of the ABA signal (Han et al., 2012). These findings combined with those from a prior study that revealed a link between the putative BRM complex component SWI3B and a core ABA signaling component, the clade A PP2C HAB1 (Saez et al., 2008), suggested the possibility that BRM activity might be controlled by ABA.

Further support for this idea came from in vivo phosphoproteomic studies. For example, a global analysis of the Arabidopsis phosphoproteome after ABA treatment in the wild type and the *snrk2.2/2.3/2.6* triple mutant identified new putative substrates of the ABA-activated SnRK2s (Umezawa et al., 2013; Wang et al., 2013). BRM phosphopeptides were identified preferentially in ABA-treated wild-type (wt) that were not detected in the

snrk2.2/2.3/2.6 triple mutant. These results suggested that BRM might be substrate of the ABA-activated SnRK2s, either directly or indirectly through activation of additional downstream kinases such as MPKs (Umezawa et al., 2013; Wang et al., 2013). Here, we provide evidence that BRM is a direct target of SnRK2s and of PP2Cs, identify conserved OST1 phosphorylation sites in the C-terminal region of BRM, which are dephosphorylated by PP2CA, and provide evidence that phosphomimetic *BRM* mutants are ABA hypersensitive. Our results reveal roles for the core ABA signaling pathway, including PYR/PYL ABA receptors, clade A PP2Cs and SnRK2s, in directly controlling a chromatin regulatory protein. Moreover, our results suggest that phosphorylation of BRM by SnRK2s is a mechanism to release BRM-mediated repression of *ABI5* expression and thus ABA response, whereas PP2C-mediated dephosphorylation of BRM likely maintains the repressive function of BRM on ABA response.

RESULTS

Genetic interaction between SnRK2.2/2.3 and BRM suggests BRM is a target of the core ABA signaling pathway

To test for a functional link between the core ABA signaling pathway and BRM, we crossed the ABA-hypersensitive *brm-3* mutant to the ABA-insensitive *snrk2.2/2.3* mutant to generate a *brm-3*/*snrk2.2/2.3* triple mutant. ABA-mediated inhibition of seedling establishment was compared among the different genetic backgrounds (Figure 1A and B). We found that the ABA-insensitive phenotype of the *snrk2.2/2.3* double mutant was attenuated when *brm-3* was introduced in this genetic background. Likewise, the reduced sensitivity of *snrk2.2/2.3* to ABA-mediated inhibition of root growth was attenuated in the *brm-3*/*snrk2.2/2.3* triple mutant (Figure 1C). These results suggest that the ABA insensitivity of *snrk2.2/2.3* is in part dependent on BRM repressing ABA response. To further test this idea we took advantage of a double mutant previously generated that combines the *brm-101* null mutant and a *35S:HAB1* overexpressing (OE) line (Saez et al., 2004, Han et al., 2012). HAB1 OE leads to enhanced dephosphorylation of SnRK2s at Ser residues of the kinase activating loop, which prevents SnRK2 activation and ABA signaling (Vlad et al., 2009;

Umezawa et al., 2009; Antoni et al., 2013) and thus phenocopies higher order *snrk2* mutants. HAB1 OE causes ABA-insensitivity in the root. The ABA-insensitive phenotype of HAB1 OE lines was attenuated in *brm-101 HAB1* OE plants (Figure 1D), which likewise suggests that HAB1 gain-of-function effect on ABA signaling is partially dependent on BRM activity.

BRM physically interacts with SnRK2s and clade A PP2Cs

BRM is a SWI/SNF subgroup ATPase and has the canonical domains found in this family of proteins (Han et al., 2015; Figure 2A). BRM has an N-terminal region with a glutamine-rich domain and a helicase SANT associated domain (HSA), which frequently serves as docking site for recruiting transcription factors such as LFY and TCP4 (Farrona et al., 2004; Szerlong et al., 2008; Wu et al., 2012; Efroni et al., 2013). This is followed by the catalytic helicase-like ATPase domain, the Snf2 ATP coupling (SnAC) domain and a C-terminal domain which contains an AT-hook and a bromodomain; these domains are important for catalytic activity of BRM and for BRM association with chromatin, respectively (Farrona et al., 2007; Sen et al., 2011; Han et al., 2015).

The genetic interaction between BRM and SnRK2s, together with data obtained in phosphoproteomic studies (Wang et al., 2013; Umezawa et al., 2013), combined with the known role of BRM in preventing ABA response in the absence of the cue (Han et al., 2012), prompted us to test whether BRM is a direct target of the core ABA signaling pathway. First, we used bifluorescence molecular complementation (BiFC) in *Arabidopsis* leaf protoplasts (Figure 2B) and in tobacco leaf epidermal cells (Figure 2C and D) to test whether BRM physically interacts with key components of the ABA signaling pathway, namely SnRK2s and clade A PP2Cs. Because BRM is a large protein (2193 amino acid residues), it is difficult to express transiently; we therefore generated translational fusions of the N-terminal 1-950 (BRM^N) and C-terminal 1541-2193 (BRM^C) residues to YFP^N. Both fusion proteins localized to the nucleus of plant cells (Supplemental Figure 1), as expected. We found that both BRM^N and BRM^C were able to interact either with the OST1/SnRK2.6 kinase or the HAB1 PP2C phosphatase in the nucleus of *Arabidopsis* protoplasts (Figure 2B). A negative control was provided by an unrelated nuclear localized protein (NC)

that lacks interaction both with HAB1 and OST1/SnRK2.6 (Figure 2B) (Wu et al., 2012). We confirmed and extended the above interaction by BiFC assays in tobacco epidermal cells and showed that SnRK2.2/2.3/2.6 kinases were able to interact with BRM^N and BRM^C (Figure 2C). SnRK2.6Δ280, which lacks the C-terminal ABA box (Vlad et al., 2009), was no not able to interact with BRM^N or BRM^C. The interaction of BRM^N with SnRK2s was confirmed by using Y2H interaction assays. The BRM^C fragment, which contains chromatin interacting domains, could not be assayed in Y2H assays because of auto-activation. Likewise, two clade A PP2Cs, PP2CA and HAB1 were able to interact with BRM^N and BRM^C on the basis of BiFC (Figure 2D). In contrast, the closely related HAI1 PP2C did not interact with BRM in BiFC assays. The interaction of BRM^N with HAB1 and PP2CA was confirmed using Y2H assays. Additionally we found that AHG1, another clade A PP2C expressed mainly in seeds, interacted with BRM^N in Y2H tests. In more stringent Y2H assay conditions (medium lacking Ade and His) we could not detect interaction between HAB1 or ABI2 and BRM^N; however, in medium lacking His and supplemented with 3AT, we could confirm the interaction of HAB1 with BRM^N (Figure 2D, right panel bottom).

In order to test whether full-length BRM protein is able to interact with SnRK2 kinases and PP2C phosphatases in plant cells, we performed co-immunoprecipitation (coIP) experiments. Firstly, we demonstrated that a fraction of SnRK2.2/2.3 and of PP2CA proteins, as well as of BRM itself, could be detected in soluble nuclear extracts (Supplemental Figure 2). Next, we transformed ProBRM:BRM-GFP plants with 35S:3HA-SnRK2.2 or 35S:3HA-PP2CA and generated stable transgenic lines. After anti-HA antibody immunoprecipitation in nuclear extracts from ProBRM:BRM-GFP 35S:3HA-SnRK2.2 plants, we tested for coIP of BRM-GFP using anti-GFP monoclonal antibody (Figure 2E). BRM was co-immunoprecipitated with SnRK2.2 in the absence or presence of ABA (50 μM for 1 h). Hence ABA-mediated activation of SnRK2.2 is not a prerequisite for its interaction with BRM. This result is in agreement with Y2H assays, which show that non ABA-activated SnRK2s are able to interact with BRM^N (Figure 2C). To test the interactions between BRM and PP2CA in plant cells, we first immunoprecipitated BRM-GFP with anti-GFP

antibodies and tested for coIP of 3HA-PP2CA using anti-HA. We detected PP2CA coIP in the absence, but not in the presence of ABA (50 μM for 1 h). In the presence of ABA, PP2CA forms a highly stable PP2C-ABA-receptor complex both in the nucleus (predominantly) and cytosol of plant cells (Pizzio et al., 2013). Thus ABA treatment impairs the interaction of PP2CA with BRM (Figure 2E), which may be the result of PP2CA being hijacked by ternary phosphatase-ABA-receptor complexes.

In vitro phospho/dephosphorylation of the carboxy-terminal region of BRM by OST1/PP2CA

Several large scale experiments have identified phosphorylation sites in BRM by mass spectrometry (The Arabidopsis Protein Phosphorylation Site Database (PhosPhAt 4.0; http://phosphat.uni-hohenheim.de/phosphat.html) (Durek et al., 2010; Wang et al., 2013; Umezawa et al., 2013). In particular, more than ten phosphopeptides in the C-terminal domain of BRM were identified following ABA treatment in the wild type that were absent in *snrk2.2/2.3/2.6* triple mutant or were induced by osmotic stress (Wang et al., 2013; Umezawa et al., 2013; Xue et al., 2013; Supplemental Table 1; Supplemental Figure 3). For example, phosphoproteomic studies identified S1760 and S1762 as putative phosphorylation targets of SnRK2.2/2.3/2.6 that lay in the well known LxRxxS consensus site for OST1 phosphorylation (Sirichandra et al., 2010; Wang et al., 2013; Umezawa et al., 2013). We reasoned that residues critical for BRM function in this region should be evolutionarily conserved. For instance, S1760 and S1762 were found to be conserved in the analysed plant genomes (Supplemental Figure 4). The C-terminal region of BRM contains domains that are critical for nucleosome interaction and normal function of BRM (Farrona et al., 2007). For instance, the potential phosphorylation sites (S1760 and S1762) are located between the AT-hook, which is a non-specific DNA binding domain rich in lysines and arginines required for tethering of BRM to chromatin (Bourachot et al., 1999) and the bromodomain, which is is known to interact with acetylated lysines of histones H3 and H4 (Dhalluin et al., 1999; Farrona et al., 2007) (Figure 2A). Further support for the importance of this domain comes from the *brm-3* allele, which carries a T-DNA insertion just upstream of the bromodomain. This insertional mutation causes formation of a truncated BRM

polypeptide lacking the last 454 residues and impairs BRM function (Farrona et al., 2007). Finally, additional potential SnRK2 phosphorylation sites are located after the bromodomain (Supplemental Table 1; Supplemental Figure 3).

To test whether BRM is a direct target of SnRK2s, we generated recombinant fragments of this chromatin remodelling ATPase for in vitro phosphorylation assays. We purified two histidine-tagged C-terminal domain fragments [BRMC2 (residues 1541-1890) and BRMC3 (residues 1891-2193)] and one N-terminal fragment as an MBP fusion protein [MBPD2 (residues 684-950), which contains the HSA domain] (Supplemental Figure 5). Next, we tested these fragments as in vitro substrates in phosphorylation assays with the OST1/SnRK2.6 kinase (Figure 3). Recombinant OST1 is 10-fold more active than SnRK2.2 and SnRK2.3 in phosphorylation assays as determined by [^{32}P]-γATP labeling (Ng et al., 2011). Fragment BRMC2, which migrates just below OST1, and fragment BRMC3 were phosphorylated in vitro by OST1 and, as previously reported (Dupeux et al., 2011; Ng et al., 2011), OST1 autophosphorylated (Figure 3A). In contrast to BRMC2 and BRMC3, the BRMD2 (684-950 residues) fragment was not phosphorylated by OST1 (Figure 3A, right panel). Addition of the PP2CA phosphatase 45 min after the phosphorylation reaction took place, led to dephosphorylation of both the OST1 and the BRM fragments (Figure 3A, left panel). However, addition of the PP2CA phosphatase together with PYL8 and ABA did not result in BRM or OST1 dephosphorylation (Figure 3A, left panel). This was expected since PYL8 inhibits PP2CA activity in an ABA-dependent manner (Antoni et al., 2012). These results suggest that ABA-mediated activation of SnRK2s initiated by PYR/PYL ABA receptors leads to phosphorylation of BRM, whereas the clade A PP2CA is able to dephosphorylate BRM when ABA levels are low.

Identification of sites phosphorylated by OST1 in the carboxy-terminal part of BRM

Next we performed in vitro cold phosphorylation of BRMC2 and BRMC3 by OST1 in order to identify by proteomic analysis the precise residues phosphorylated. After incubation of BRMC2 and BRMC3 with OST1, phosphopeptides were enriched by Immobilized Metal Affinity Chromatography

(IMAC) and Oligo R3 reversed-phase chromatography (Navajas et al., 2011). Phosphopeptide analysis was performed using CID/ETD fragmentation of the most abundant ions and liquid chromatography-tandem mass spectrometry (LC-MS/MS) (Navajas et al., 2011). For protein identification, CID and ETD spectra obtained by LC–MS/MS system were searched against the SwissProt database using a licensed version v.2.3.02 of Mascot (Matrix Science, London, UK) as search engine. Using this strategy we identified one phosphopeptide in BRMC2: SGpS^{1762}WAHDR, and three phosphopeptides in BRMC3: NALSFSGSAPTLVS(T)^{2029}P(T)^{2031}PR, TGGS(S)^{2120}(S)^{2121}PVSPPPA MIGR and SPVpS^{2139}GGVPR, whose CID/ETD spectra are provided in Figure 3B. The fragmentation pattern of some of the phosphorylated peptides in the CID/ETD spectra did not allow the unambiguous assignment of the phosphate group to specific S/T residues (in brackets). In these cases, the peptide sequence and the number of phosphorylation sites in the peptide could be derived from the mass spectrum, but not the precise location within the sequence. However, for the SGpS^{1762}WAHDR and SPVpS^{2139}GGVPR phosphorylated peptides, the precise location of the phosphorylation site was derived from the mass spectrum.

The 4 BRM phosphopeptides identified here matched those deposited in PhosPhAt database based on in vivo phosphoproteomics (Durek et al., 2011; Supplemental Figure 3). In particular, the genetic-phosphoproteomic studies performed by Wang et al., (2013) and Umezawa et al., (2013) yielded BRM phosphopeptides that matched those identified in our in vitro analysis (Supplemental Table 1). However, those studies did not discern whether the identified BRM phosphopeptides were a direct target of SnRK2s or downstream targets of MAPKs/GSKs that might be dependent on SnRK2 function (Umezawa et al., 2013). Motif analysis of ABA-responsive phosphopeptides has identified four groups of motifs (Umezawa et al., 2013). Motif analysis of the phosphorylated BRM peptides identified in our assays revealed that SGpS^{1762}WAHDR matched motif 1: (K/R)xx(pS/pT), whereas SPVpS^{2139}GGVPR matched motif 4: (S)xx(pS). The LQRSGS^{1762}WAHDR peptide moreover matches a well known LxRxxS consensus site for OST1 phosphorylation (Sirichandra et al., 2010), and phosphorylation of both Ser1760

and Ser1762 was found in BRM phosphopeptides present in PhosPhAt 4.0 (Wang et al., 2013; Umezawa et al., 2013). The phosphopeptides TGGS(S)^{2120}(S)^{2121}PVSPPPAMIGR, NALSFSGSAPTLVS(T)^{2029}PTPR and SPVpS^{2139}GGVPR match motif 3 (pS/T-P; pSxP; pSPxpS) and we found in PhosPhAt 4.0 evidence for in vivo existence of the corresponding phosphopeptides (Wang et al., 2013; Umezawa et al., 2013; Supplemental Table 1; Supplemental Figure 3). In addition to the OST1 phosphorylation sites identified in this study, other putative SnRK2 phosphorylation sites, for instance EIEDDIAGYpS^{1629}EEpS^{1632}pS^{1633}EERNIDpS^{1640}NEEE, were previously identified in the C-terminus of BRM that match the [acidic pS acidic] consensus (Wang et al., 2013; Umezawa et al., 2013). In summary, our in vitro phosphorylation assays together with in vivo phosphoproteomic studies indicate that BRM C-terminus is a hotspot for ABA-dependent phosphorylation (Supplemental Table 1; Supplemental Figure 3). We also provide direct evidence that OST1 is able to phosphorylate Ser1762 and Ser2139 residues, and either S2120/S2121 or T2029/2031 in the C-terminal part of BRM.

PYL ABA receptors impair the interaction of PP2CA with BRM

Our *in vitro* results indicated PP2CA was able to dephosphorylate the C-terminal region of BRM after its phosphorylation by OST1 only when PP2CA was not complexed with PYL8 in the presence of ABA (Figure 3A). Moreover, *in planta* ABA-treatment was able to prevent co-immunoprecipitation of PP2CA with full-length BRM (Figure 2D). These data prompted us to examine whether ABA and PYL ABA receptors modulate the direct interaction between BRM and PP2CA. Towards this end we employed a yeast three-hybrid approach (Brachmann and Boeke, 1997). The interaction between GBD-BRMN and GAD-PP2CA was disrupted in an ABA-dependent manner by the presence of PYL4 or PYL5 (Figure 4A). ABA itself did not affect the interaction of BRM^{N} and a well known partner of BRM, i.e. the SWI3C subunit of the SWI/SNF chromatin remodelling complex (Hurtado et al., 2006; Jerzmanowski, 2007) (Figure 4A).

We also examined whether the interaction of SnRK2.3 with BRM was disrupted by the presence of PP2CA, which has been reported to interact with SnRK2.3 in Y2H assays (Umezawa et al., 2009). The presence of PP2CA did

not disrupt the BRM-SnRK2.3 interaction (Figure 4B). These results suggest that under basal low ABA levels, where PP2Cs are not forming stable ternary complexes with PYR/PYLs, the presence of free PP2C might not affect the interaction between SnRK2 and BRM, in agreement with the coIP results obtained in Figure 2D. Under these conditions, however, the activation loop of SnRK2s is not phosphorylated and hence the kinase is not active (Fujii et al., 2009)

BRM $^{S1760D\ S1762D}$ phosphomimetics display ABA-hypersensitivity and increased *ABI5* expression

Because BRM represses ABA response during germination in large part by preventing *ABI5* expression in the absence of ABA (Han et al., 2012), we hypothesized that phosphorylation of BRM by SnRK2s -key positive regulators of ABA signaling- might lead to inactivation of BRM and activation of ABA response. Direct biochemical assay of BRM chromatin remodeling activity in the phosphorylated and non-phosphorylated form was not feasible because we could not obtain sufficient recombinant protein, either by expression in *E. coli* or insect cells using baculovirus vector, to test in vitro remodeling activity. As an alternative approach to test the effect of SnRK2 phosphorylation on BRM activity and taking advantage of the phosphorylation sites identified, we designed a BRM phosphomimetic mutant where Serine (S) residues were replaced by Aspartic acid (D). Negatively charged amino acids such as Asp or Glu can frequently mimic the effect of phosphorylated serine (Konson et al., 2011). A BRM$^{S1760D\ S1762D}$ phosphomimetic mutant was generated and introduced into the *brm-3* background. Analysis of ABA-mediated inhibition of seed germination and seedling establishment revealed that transgenic lines expressing BRM$^{S1760D\ S1762D}$ were ABA hypersensitive compared to wild type (Figure 4C). BRM$^{S1760A\ S1762A}$ phosphomutant transgenic plants in the *brm-3* background, or BRM^{WT} in a *brm* mutant background, by contrast, did not display ABA hypersensitivity (Figure 4C and 4D). Moreover, expression of *ABI5* was elevated in BRM phosphomimetic mutant lines, relative to the wild type (Figure 4E). These results are consistent with the idea that phosphorylation of BRM leads to release of its inhibitory effect on *ABI5* expression (Figure 4F).

Conversely, these results suggest that PP2C-mediated dephosphorylation of BRM serves to maintain its repressive effect on *ABI5* expression.

DISCUSSION

The SWI/SNF ATPase BRM represses ABA responses in the absence of stress to balance plant growth and stress response (Han et al., 2012). Both the *brm-1* and *brm-3* loss-of-function alleles show enhanced ABA-mediated inhibition of seedling establishment, this defect is rescued by removal of *ABI5*. BRM represses *ABI5* expression in the absence of the stress signal by stabilizing a nucleosome close to the *ABI5* transcription start site (Han et al., 2012). Although BRM does not prevent ABA-mediated destabilization of this nucleosome, it still resides at the *ABI5* locus in conditions of elevated ABA. This raised the possibility that BRM might be inactivated in the presence of ABA – for example by a posttranslational modification (Han et al., 2012). In this work, we provided evidence to propose a model where ABA/SnRK2-mediated phosphorylation impairs BRM activity (BRM OFF), which releases BRM repression and leads to induction of *ABI5* (Figure 4E). Conversely, PP2C-mediated dephosphorylation restores BRM activity (BRM ON) to maintain repression of ABA responses (and *ABI5* expression) under normal plant growth conditions.

ABA signalling relies on a phosphorylation cascade and analysis of the phosphoproteome in response to ABA had suggested that BRM might be phosphorylated by SnRK2s. In this work we provide direct evidence that OST1 is able to phosphorylate at least four Ser/Thr residues in the C-terminal region of BRM and that introduction of two phosphomimetic S1760D S1762D mutations impairs BRM function. Moreover, we have established that both SnRK2s and PP2Cs interact with the N- and C-terminal domains of BRM and co-immunoprecipitate with full-length BRM in the absence of exogenous ABA. Interestingly, whereas ABA-treatment did not significantly affect the interaction of SnRK2 and BRM, this treatment dramatically reduced the interaction between PP2CA and BRM. These results were corroborated by yeast two- and three-hybrid analyses. Thus, ABA perception through PYR/PYL ABA receptors

may abrogate the PP2CA interaction with BRM (Figure 4A and model Figure 4E).

ABA leads to phosphorylation of the activation loop of SnRK2s, which is a requisite for activation of the kinase (Umezawa et al., 2009; Vlad et al., 2010). We have demonstrated that recombinant autophosphorylated OST1/SnRK2.6 is able to phosphorylate the C-terminal region of BRM. This region, according to the high number of SnRK2-dependent phosphopeptides identified in PhosPhAt (Wang et al., 2013; Umezawa et al., 2013), seems to be a hotspot for ABA-dependent phosphorylation. What effect on BRM activity could be expected from this phosphorylation? In the absence of a biochemical assay for BRM activity, we relied on the generation of a phosphomimetic mutant, BRM $^{S1760D\ S1762D}$, which was introduced in the hypomorphic *brm-3* allele. The *pBRM:BRM* $^{S1760D\ S1762D}$*::brm-3* mutant showed enhanced ABA sensitivity compared to the wt. Moreover, the *pBRM:BRM* $^{S1760D\ S1762D}$*::brm-3* mutant displayed increased *ABI5* expression, which suggests that irreversible introduction of negative charge in certain Ser residues of BRM impairs its function in ABA signaling. ABA treatment led to a similar fold increase in the wild type, in *brm*-3 and in *pBRM:BRM* $^{S1760D\ S1762D}$*::brm-3*, consistent with the prior conclusion that BRM is inactivated upon ABA sensing (Han et al., 2012).

The combined data point to a model (Figure 4E) where reversible phosphorylation of BRM by SnRK2s might lead to transient inactivation of the ATPase, which could be reverted by PP2CA. Our results also suggest that ABA-mediated induction of *ABI5* requires phosphorylation of BRM by ABA-activated SnRK2s. Once the ABA levels diminish when plants return to non-stress conditions, PP2CA might dephosphorylate BRM to restore its activity and allow BRM to repress *ABI5* expression. *Arabidopsis* mutants lacking PP2CA or HAB1 show enhanced ABA-mediated inhibition of germination and seedling establishment and higher expression of *ABI5* than wt (Nishimura et al., 2007; Rubio et al., 2009), which is in agreement with a role of PP2CA/HAB1 in maintaining BRM activity for repression of *ABI5* expression.

The in vivo identified SnRK2-dependent phosphorylation sites were concentrated around the AT hook and Bromodomain of BRM, which are

important domains for BRM function (Farrona et al., 2007). These domains constitute a module that allows BRM to interact with linker and nucleosomal DNA as well as the histone octamer (Farrona et al., 2007). The domains are required for BRM function since the *brm-3* mutant, which lacks most of this module (yet retains the AT-hook), behaves as a hypomorphic allele (Farrona et al., 2007). In contrast, no phosphorylation sites were found in other important regions of BRM, such as the ATPase region required for ATP hydrolysis or the SnAC domain, which couples ATP hydrolysis to nucleosome movement (Sen et al., 2011, 2013). Therefore, we suggest that the C-terminal region located after the AT-hook domain and the bromodomain represents a hotspot for regulation through phosphorylation/dephosphorylation events. Interestingly, human BRM and BRG1 are phosphorylated and excluded from the condensed chromosomes during mitosis (Muchardt et al., 1996). Numerous phosphorylated serine/threonine residues were identified before and after the bromodomain of the human BRM and BRG1 proteins (PhosphositePlus; http://www.phosphosite.org/proteinAction.do?id=5848&showAllSites=true).

Therefore, phosphorylation of the C-terminal domain of BRM may be evolutionary conserved. In the case of *Arabidopsis* BRM, the phosphomimetic $BRM^{S1760D\ S1762D}$ mutant phenocopies ABA-hypersensitivity of *brm* loss-of-function alleles, which strongly suggests that SnRK2-dependent phosphorylation releases BRM repression of ABA signaling. Conversely, PP2CA and HAB1, which are key negative regulators of ABA signaling, cooperate to maintain dephosphorylated and active BRM in the absence of the cue. In summary, our work provides a direct link between the core ABA signaling pathway and the chromatin remodeling ATPase BRM. This link enables ABA-dependent modulation of BRM activity and a possible entry point for increasing response to water stress in plants.

METHODS

Plant material and growth conditions

Arabidopsis thaliana plants were grown as described by Pizzio et al., (2013). The *brm-3* and *snrk2.2/2.3* mutants have been described previously (Farrona et al., 2007; Fujii et al., 2007). The GFP-tagged version of BRM (pBRM:BRM-GFP) in *brm-1* background has been described previously (Han et al., 2012; Wu et al., 2015). The HA-tagged versions of PP2CA and SnRK2.2/2.3 in wt background have been described previously (Antoni et al., 2012; Planes et al., 2015). The *brm-3* allele was crossed with the *snrk2.2/2.3* double mutant to generate a *brm-3 snrk2.2/2.3* triple mutant. The pBRM:BRM-GFP line was transformed with either the pAlligator2-HA-PP2CA or HA-SnRK2.2 constructs to generate lines containing both GFP- and HA-tagged versions of BRM and PP2CA or BRM and SnRK2.2, respectively. The pALLIGATOR2 constructs were transferred to *Agrobacterium tumefaciens* C58C1 (pGV2260) (Deblaere *et al.,* 1985) by electroporation and used to transform the pBRM:BRM-GFP line by the floral dip method (Clough and Bent, 1998). T1 transgenic seeds were selected based on GFP visualization and sowed in soil to obtain the T2 generation. Homozygous T3 progeny was used for further studies and expression of HA-tagged protein was verified by immunoblot analysis using anti-HA-peroxidase (Roche). Expression of BRM-GFP was visualized using CLSM and verified by immunoblot analysis of nuclear extracts prepared as described by Antoni et al., (2012). PCR-mediated genotyping of the different genetic backgrounds was done using the primers described in Supplemental Table 2 online.

Transient protein expression in *Nicotiana benthamiana*, *Arabidopsis* protoplasts and BiFC assays

Agrobacterium infiltration of tobacco leaves was performed basically as described by Voinnet et al., (2003). Constructs to investigate the subcellular localization of BRM^N and BRM^C proteins were done in pMDC83 vector. To investigate the interaction of either BRM^N or BRM^C and components of the core ABA signalling pathway, we used the pSPYNE-35S, pSPYCE-35S, YFP^N43 and $pYFP^C43$ vectors (Walter et al., 2004; Belda-Palazon et al., 2012). The BRM^N or

BRM^C coding sequences were cloned into pCR8/GW/TOPO entry vector and recombined by LR reaction into pSPYNE-35S or pSPYCE-35S. The coding sequences of SnRK2.2/2.3/2.6 or PP2CA/HAB1/HAI1 were recombined by LR reaction from pCR8 entry vectors to $pYFP^C43$ or YFP^N43 destination vectors, respectively. The different binary vectors described above where introduced into *Agrobacterium tumefaciens* C58C1 (pGV2260) (Deblaere et al., 1985) by electroporation and transformed cells were selected in LB plates supplemented with kanamycin (50 mg/L). Then, they were grown in liquid LB medium to late exponential phase and cells were harvested by centrifugation and resuspended in 10 mM morpholinoethanesulphonic (MES) acid-KOH pH 5.6 containing 10 mM MgCl2 and 150 mM acetosyringone to an OD600 nm of 1. These cells were mixed with an equal volume of *Agrobacterium* C58C1 (pCH32 35S:p19) expressing the silencing suppressor p19 of tomato bushy stunt virus (Voinnet et al., 2003) so that the final density of *Agrobacterium* solution was about 1. Bacteria were incubated for 3 h at room temperature and then injected into young fully expanded leaves of 4-week-old *Nicotiana benthamiana* plants. Leaves were examined 48-72 h after infiltration using confocal laser scanning microscopy.

Arabidopsis protoplast isolation and transformation was performed as described by Yoo *et al.,* (2007). BiFC assays tested the interaction of BRM^N or BRM^C (in pSPYNE(R)173) with either HAB1 or OST1 (in pSPYCE(MR)) by co-transformation of pSPYNE/pSPYCE constructs into protoplasts (Waadt *et al.,* 2008).

Yeast two-hybrid and triple-hybrid assays

BRM^N was fused by Gateway recombination to the GAL4 DNA-binding domain (GBD) or GAL4 transcriptional activation domain (GAD) in pGBKT7GW or pGADT7GW, respectively. The SnRK2.2/2.3/2.6 proteins were fused to the GBD in pBridge or pGBT9 vectors, whereas clade A PP2Cs were fused to the GAD in pGADT7 as described previously (Fujii et al., 2009). Interaction assays were usually performed as described by Saez et al. (2008), using the AH109 yeast strain and testing yeast growth in medium lacking His and Ade. To detect the BRM^N-HAB1 interaction, BRM^N in pDEST32 (BD) and HAB1 in pDEST22

(AD) vector were co-transformed into PJ69-4A yeast strain. The resulting transformants were grown overnight in liquid -Trp-Leu/SD medium and adjusted to equal cell density. Serial dilutions of cells were spotted on -Trp-Leu-His/SD medium with 0.1 mM of 3-amino-1, 2, 4-triazole (3-AT). To perform triple-hybrid experiments where ABA receptors interfere with the binding of PP2CA to BRM^N, the sequence of BRM^N was fused to GBD in pBridge. Next, the coding sequences of PYL4 or PYL5 were cloned into the *Not*I site (multicloning site II, abbreviated as MCSII) of pBridge-BRM^N. For triple-hybrid experiments with PP2CA and SnRK2.3, the sequence of SnRK2.3 was firstly fused to GBD in pBridge. Next, the coding sequence of PP2CA was cloned into the *Not*I site of pBridge-SnRK2.3.Yeast growth in triple-hybrid experiments was tested either in medium lacking His supplemented with 3-AT (Figure 4A) or medium lacking His and Ade (Figure 4B).

Confocal Laser Scanning Microscopy

Confocal imaging was performed using a Zeiss LSM 780 AxioObserver.Z1 laser scanning microscope with C-Apochromat 40x/1.20 W corrective water immersion objective. The following fluorophores, which were excited and fluorescence emission detected by frame switching in the single or multi-tracking mode at the indicated wavelengths, were used in tobacco leaf infiltration experiments: GFP (488 nm/500-530 nm) and YFP (488 nm/529-550 nm). Pinholes were adjusted to 1 Air Unit for each wavelength. Post-acquisition image processing was performed using ZEN (ZEISS Efficient Navigation) Lite 2012 imaging software and ImageJ (http://rsb.info.gov/ij/).

To quantify relative fluorescence intensities of BiFC experiments, all images were captured using the same laser, pinhole and gain settings of the confocal microscope to maintain high reproducibility of the dates (laser 2.0%, pinhole diameter 34 µm, master gain 740, digital gain 1.00, digital offset 0.00), as well as zoom factor (1.2) covering 2-3 living cells/image. As negative controls in the interaction assays, *Agrobacterium* expressing BRM^N-YFPN was co-infiltrated with YFP^C-SnRK2.10 (Vlad et al., 2009) and BRM^N-YFPC was co-infiltrated with YFP^N-HAI1. Image quantification of relative fluorescence intensities was carried out using ImageJ software by measuring the fluorescence intensity corrected for mean background fluorescence subtracted

from corresponding areas showing no green fluorescence. Each BiFC experiment was scanned and measured in 25 randomly chosen microscopic fields (n=25) and repeated tree times.

Biochemical fractionation, protein extraction, analysis and immunoprecipitation

Protein extracts for immunodetection experiments were prepared from tobacco leaves 48-72 h after infiltration or from Arabidopsis transgenic lines expressing GFP- and HA-tagged versions of BRM and PP2Cs/SnRK2s, respectively. Plant material (~100 mg) for direct Western blot analysis was extracted in 2X Laemmli buffer (125 mM Tris-HCl pH 6.8, 4% SDS, 20% glycerol, 2% mercaptoethanol, 0.001% bromophenol blue), proteins were run in a 4-15% SDS-PAGE MiniProtean precast gel (BioRad) and analyzed by immunoblotting. Nuclear fractionation of GFP- or HA-tagged proteins was performed as described previously (Saez et al., 2008; Antoni et al., 2012) and the soluble nuclear fraction was used for immunoprecipitation experiments. Soluble proteins from the nuclear fraction were immunoprecipitated using super-paramagnetic micro MACS beads coupled to monoclonal anti-GFP or anti-HA antibody according to the manufacturer´s instructions (Miltenyi Biotec). Purified immunocomplexes were eluted in Laemmli buffer, boiled and run in a 10% SDS-PAGE gel. Proteins immunoprecipitated with anti-GFP antibody were transferred onto Immobilon-P membranes (Millipore) and probed with anti-HA-peroxidase to detect coIP of HA-tagged PP2CA. On the other hand, proteins immunoprecipitated with anti-HA antibody were probed with anti-GFP to detect coIP of GFP-tagged BRM. Immunodetection of GFP fusion proteins was performed with an anti-GFP monoclonal antibody (clone JL-8, Clontech) as primary antibody and ECL anti-mouse-peroxidase (GE Healthcare) as secondary antibody. Antibodies were used to a 1:10000 dilution. Detection was performed using the ECL advance western blotting chemiluminiscent detection kit (GE Healthcare). Image capture was done using the image analyzer LAS3000 and quantification of the protein signal was done using Image Guache V4.0 software.

Protein preparation

Purification of OST1, PP2CA and PYL8 recombinant proteins was performed as described previously (Santiago et al., 2009; Antoni et al., 2012). BRM protein fragments corresponding to the C-terminal region, BRMC2 (1541-1890) and BRMC3 (1891-2193), were amplified using PCR and cloned into pETM11. Expression of each recombinant protein in *Escherichia coli* BL21 (DE3) cells transformed with the corresponding pET28a/pETM11 construct was induced using 1 mM IPTG and 6His-tagged recombinant proteins were purified to homogeneity using Ni-NTA affinity chromatography (Antoni et al., 2012). We also generated a pMalc2-BRMD2 (684-950) construct and expression of the encoded MBP-D2 fusion protein was induced in *E. coli* DH5a cells using 1 mM IPTG. Purification of MBP-D2 was performed using amilose affinity chromatography.

In vitro phosphorylation of BRM by OST1 and phosphopeptide proteomic analysis

Phosphorylation assays were done basically as described previously (Dupeux et al., 2011). Briefly, a reaction mixture containing 1 μg 6His-OST1 and 1 μg of either 6His-BRMC2, 6His-BRMC3 or MBP-BRMD2 was incubated for 60 min at room temperature in 30 μl kinase buffer: 20 mM Tris-HCl pH 7.8, 10 mM MgCl2, 2 mM MnCl2, 0.5 mM DTT and 3.5 μCi of γ-^{32}ATP (3000 Ci/mmol). When indicated, ABF2ΔC recombinant protein (100 ng) was added as a substrate of OST1. Reactions were stopped by adding Laemmli buffer, proteins were separated by SDS/PAGE using an 8% (w/v) acrylamide gel, transferred to an Immobilon-P membrane and detected using a phosphorimage system (FLA5100; Fujifilm, Tokyo, Japan).

Cold phosphorylation of 6His-BRMC2 and 6His-BRMC3 substrates was performed in the presence of 1 mM ATP. Next, samples were run on a 1D gel, Coomassie stained and the gel bands corresponding to the different proteins were cut and in-gel digested. Briefly, following reduction and alkylation (10 mM and 50 mM DTT and iodoacetamide respectively, both in 25 mM ammonium bicarbonate), BRMC2 and BRMC3 samples were digested with trypsin (1:50 enzyme-to-protein ratio) and incubated overnight at 37°C. Peptides were

recovered in 50% ACN/ 1% TFA, dried in speed-Vac and kept at -20°C until phosphopeptide enrichment. The enrichment procedure concatenated two in-house packed microcolumns, the IMAC microcolumn and the Oligo R3 reversed-phase one, which provides selective purification and sample cleanup prior to LC-MS/MS analysis. Reversed-phase liquid chromatography was performed on an Ultimate 3000 nanoHPLC (Dionex, Amsterdam, The Netherlands). A 5μL volume of the reconstituted peptide samples was injected on a C18 PepMap trap column (5μm, 100 Å, 300 μm I.D. x 5mm) at a flow rate of 30 μL/min, using H2O:AcN:TFA (98:2:0.1) as loading mobile phase for 5 min. Then, the trap column was switched on-line in back-flush mode to a C18 PepMap 100 analytical column (3μm, 100 Å, 75 μm I.D. x15 cm). A 60 min linear gradient of 4% - 50% B was delivered from the micro pump at a flow rate of 300 nL/min, where mobile phase A was 0.1% formic acid in water and B was 20% water, 0.1% formic acid in acetonitrile. For rinsing the column, the percentage of B was increased to 95% in 6 min and then, returned to initial conditions in 2 min. Afterwards the column was re-equilibrated for 15 min. The UV detector wavelengths were monitored at 214 nm and 280 nm.

NanoHPLC was coupled to a 3D ion trap mass spectrometer Amazon speed (Bruker Daltoniks, Bremen, Germany) via CaptiveSpray ion source operating in positive ion mode, with capillary voltage set at 1.3 kV. The ion trap mass spectrometer was operated in a data-dependent mode, performing full scan (m/z 350-1500) MS spectra followed by tandem MS, alternating CID/ETD fragmentation of the 8 most abundant ions. Dynamic exclusion was applied to prevent the same m/z from being isolated for 1 min after its fragmentation. For protein identification, CID and ETD spectra obtained by LC–MS/MS system were searched against the SwissProt database using a licensed version v.2.3.02 of Mascot (Matrix Science, London, UK) as search engine. ETD preserves the phosphoryl moiety during peptide fragmentation which facilitates phospho-site characterization. Peptides with scores above a threshold that indicates a reliable identification were selected, and based on these individual scores protein identifications were assigned. In addition, manual validation of phosphopeptide MS/MS spectra was performed.

Seed germination and seedling establishment assays.

After surface sterilization of the seeds, stratification was conducted in the dark at 4ºC for 3 d. Approximately 100 seeds of each genotype were sowed on MS plates supplemented with different ABA concentrations per experiment. To score seed germination, radical emergence was analyzed at 72 h after sowing. Seedling establishment was scored as the percentage of seeds that developed green expanded cotyledons and the first pair of true leaves at 5 or 7 d.

Root growth assays.

Seedlings were grown on vertically oriented MS plates for 4 to 5 days. Afterwards, 20 plants were transferred to new MS plates lacking or supplemented with the indicated concentrations of ABA. The plates were scanned on a flatbed scanner after 10-d to produce image files suitable for quantitative analysis of root growth using the NIH software ImageJ v1.37.

Generation of phosphomimetic and phosphomutant BRM versions

A part of genomic gBRM fragment (*Bam*HI-*Eag*I, 2850 bp) was cloned into pENTR3C vector (Invitrogen). The S1760 and S1762 residues were mutated either to aspartic acid (phosphomimetic) or alanine (phosphomutant) by site-directed mutagenesis. To this end, we used primers described in Supplemental Table 2 following http://openwetware.org/wiki/Knight:Site-directed_mutagenesis/Single_site and Stratagene QuickChange Site-Directed Mutagenesis manual. After verification of the mutagenesis by nucleotide sequencing, the *Bam*HI-*Eag*I genomic BRM fragment containing the S1760D/A and S1762D/A changes replaced the wt fragment in pBRM::gBRM-GFP (Wu *et al.,* 2012). Subsequently, pBRM::gBRM-GFP was recombined into pGWB1 (Nakagawa *et al.,* 2007) by LR reaction (Invitrogen). The resulting binary vector was shuttled into *Agrobacterium* strain GV3101 and introduced into *brm-3* mutants via floral dip (Clough and Bent, 1998). Seeds were harvested from wt looking T1 plants. T2 and T3 lines were used for seedling establishment and *ABI5* expression assay.

Analysis of *ABI5* expression

Two-day-old seedlings that were mock or 50 μM ABA-treated for 1 h were used for *ABI5* expression analysis. RNA was extracted using TRIZOL reagent (Invitrogen) and further purified through DNaseI treatment and the RNA purification RNeasy mini kit (Qiagen). cDNA was synthesized using the Superscript IV kit (Invitrogen). Real-time PCR (StepOnePlus Real-Time PCR system-Applied Biosystems) was performed using Power SYBR Green PCR master mix (life technologies) and platinum *Taq* DNA polymerase (Invitrogen). *ABI5* transcript levels were normalized over that of the *UBQ10* gene.

Author contributions

MP-L conducted genetic studies with *brm-3* and *snrk2.2/2.3* mutants, performed BiFC studies in *Nicotiana*, together with LR and BB-P, Y2H and Y3H assays, generation of double transgenic lines and immunoprecipitation assays in Rodriguez lab. MP-L and MG-G conducted phosphorylation assays and identification of BRM phosphorylation sites following proteomic analysis; MG-G generated HA-tagged SnRK2.2 line in Rodriguez lab. SKH conducted the genetic studies with the HAB1 overexpression line, and designed, generated and performed the first analyses of the phosphomutant and phosphomimetic BRM transgenic lines as well as Y2H and Y3H studies in the Wagner lab. CWJ conducted in depth analyses of the morphological and molecular phenotypes of the phosphomimetic and phosphomutant lines in the Wagner lab. SKH and MP-L together performed BiFC studies in protoplasts, *ABI5* expression studies, yeast interaction studies and studied the ABA sensitivity of the BRM phosphomutant and phosphomimetic lines in the Wagner lab. PLR and DW each designed the experiments executed in the respective laboratories and wrote the manuscript with input from all authors.

SUPPLEMENTAL INFORMATION

Supplemental information is available at *Molecular Plant Online*

FUNDING

Work in Dr Rodriguez' s laboratory was supported by the Ministerio de Ciencia e Innovacion, Fondo Europeo de Desarrollo Regional and Consejo Superior de Investigaciones Cientificas (grant BIO2014-52537-R). MP-L and LR were supported by FPI fellowships and MG-G by a JAE-DOC research contract. Funding of chromatin research in the Wagner lab is supported by National Science Foundation grant MCB-0925071.

Acknowledgments

We acknowledge Dr. Rosana Navajas (Centro Nacional de Biotecnologia, Madrid) for help with phosphoproteomic studies.

REFERENCES

Antoni,R., Gonzalez-Guzman,M., Rodriguez,L., Rodrigues,A., Pizzio,G.A. and Rodriguez,P.L. (2012). Selective Inhibition of Clade A Phosphatases Type 2C by PYR/PYL/RCAR Abscisic Acid Receptors. Plant Physiol **158**:970-980.

Antoni,R., Gonzalez-Guzman,M., Rodriguez,L., Peirats-Llobet,M., Pizzio,G.A., Fernandez,M.A., De Winne,N., De Jaeger,G., Dietrich,D., Bennett,M.J. and Rodriguez,P.L. (2013). PYRABACTIN RESISTANCE1-LIKE8 plays an important role for the regulation of abscisic acid signaling in root. Plant Physiol **161**:931-941.

Belda-Palazon,B., Ruiz,L., Marti,E., Tarraga,S., Tiburcio,A.F., Culianez,F., Farras,R., Carrasco,P. and Ferrando,A. (2012). Aminopropyltransferases involved in polyamine biosynthesis localize preferentially in the nucleus of plant cells. PLoS One **7**:e46907.

Bourachot,B., Yaniv,M. and Muchardt,C. (1999). The activity of mammalian brm/SNF2alpha is dependent on a high-mobility-group protein I/Y-like DNA binding domain. Mol. Cell Biol. **19:**3931-3939.

Brachmann,R.K. and Boeke,J.D. (1997). Tag games in yeast: the two-hybrid system and beyond. Curr. Opin. Biotechnol. **8**:561-568.

Chinnusamy,V. and Zhu,J.K. (2009). Epigenetic regulation of stress responses in plants. Curr. Opin. Plant Biol. **12**:133-139.

Clough,S.J. and Bent,A.F. (1998). Floral dip: a simplified method for Agrobacterium-mediated transformation of Arabidopsis thaliana. Plant J. **16**:735-743.

Cutler,S.R., Rodriguez,P.L., Finkelstein,R.R. and Abrams,S.R. (2010). Abscisic acid: emergence of a core signaling network. Annu. Rev. Plant Biol. **61**:651-679.

Deblaere,R., Bytebier,B., De Greve,H., Deboeck,F., Schell,J., Van Montagu,M. and Leemans,J. (1985). Efficient octopine Ti plasmid-derived vectors for Agrobacterium-mediated gene transfer to plants. Nucleic Acids Res. **13**:4777-4788.

Dhalluin,C., Carlson,J.E., Zeng,L., He,C., Aggarwal,A.K. and Zhou,M.M. (1999). Structure and ligand of a histone acetyltransferase bromodomain. Nature **399**:491-496.

Dupeux,F., Antoni,R., Betz,K., Santiago,J., Gonzalez-Guzman,M., Rodriguez,L., Rubio,S., Park,S.Y., Cutler,S.R., Rodriguez,P.L. and Marquez,J.A. (2011). Modulation of Abscisic Acid Signaling in Vivo by an Engineered Receptor-Insensitive Protein Phosphatase Type 2C Allele. Plant Physiol **156**:106-116.

Durek,P., Schmidt,R., Heazlewood,J.L., Jones,A., MacLean,D., Nagel,A., Kersten,B. and Schulze,W.X. (2010). PhosPhAt: the Arabidopsis thaliana phosphorylation site database. An update. Nucleic Acids Res. **38**:828-834.

Efroni,I., Han,S.K., Kim,H.J., Wu,M.F., Steiner,E., Birnbaum,K.D., Hong,J.C., Eshed,Y. and Wagner,D. (2013). Regulation of leaf maturation by chromatin-mediated modulation of cytokinin responses. Dev. Cell **24**:438-445.

Farrona,S., Hurtado,L., Bowman,J.L. and Reyes,J.C. (2004). The Arabidopsis thaliana SNF2 homolog AtBRM controls shoot development and flowering. Development **131**:4965-4975.

Farrona,S., Hurtado,L. and Reyes,J.C. (2007). A nucleosome interaction module is required for normal function of Arabidopsis thaliana BRAHMA. J. Mol. Biol. **373**:240-250.

Finkelstein,R. (2013). Abscisic Acid synthesis and response. Arabidopsis Book **11**:e0166.

Fujii,H., Verslues,P.E. and Zhu,J.K. (2007). Identification of two protein kinases required for abscisic acid regulation of seed germination, root growth, and gene expression in Arabidopsis. Plant Cell **19**:485-494.

Fujii,H., Chinnusamy,V., Rodrigues,A., Rubio,S., Antoni,R., Park,S.Y., Cutler,S.R., Sheen,J., Rodriguez,P.L. and Zhu,J.K. (2009). In vitro reconstitution of an abscisic acid signalling pathway. Nature **462**:660-664.

Han,S.K., Sang,Y., Rodrigues,A., Wu,M.F., Rodriguez,P.L. and Wagner,D. (2012). The SWI2/SNF2 chromatin remodeling ATPase BRAHMA represses abscisic acid responses in the absence of the stress stimulus in Arabidopsis. Plant Cell **24**:4892-4906.

Han,S.K. and Wagner,D. (2014). Role of chromatin in water stress responses in plants. J. Exp. Bot. **65**:2785-2799.

Han,S.K., Wu,M.F., Cui,S. and Wagner,D. (2015). Roles and activities of chromatin remodeling ATPases in plants. Plant J. **83**:62-77.

Hurtado,L., Farrona,S. and Reyes,J.C. (2006). The putative SWI/SNF complex subunit BRAHMA activates flower homeotic genes in Arabidopsis thaliana. Plant Mol. Biol. **62**:291-304.

Jerzmanowski,A. (2007). SWI/SNF chromatin remodeling and linker histones in plants. Biochim. Biophys. Acta **1769**:330-345.

Konson,A., Pradeep,S., D'Acunto,C.W. and Seger,R. (2011). Pigment epithelium-derived factor and its phosphomimetic mutant induce JNK-dependent apoptosis and p38-mediated migration arrest. J. Biol. Chem. **286**:3540-3551.

Luo,M., Wang,Y.Y., Liu,X., Yang,S., Lu,Q., Cui,Y. and Wu,K. (2012). HD2C interacts with HDA6 and is involved in ABA and salt stress response in Arabidopsis. J. Exp. Bot. **63**:3297-3306.

Ma,Y., Szostkiewicz,I., Korte,A., Moes,D., Yang,Y., Christmann,A. and Grill,E. (2009). Regulators of PP2C Phosphatase Activity Function as Abscisic Acid Sensors. Science **324**: 1064-1068.

Muchardt,C., Reyes,J.C., Bourachot,B., Leguoy,E. and Yaniv,M. (1996). The hbrm and BRG-1 proteins, components of the human SNF/SWI complex, are phosphorylated and excluded from the condensed chromosomes during mitosis. EMBO J. **15**:3394-3402.

Minkoff,B.B., Stecker,K.E. and Sussman,M.R. (2015). Rapid Phosphoproteomic Effects of Abscisic Acid (ABA) on Wild-Type and ABA Receptor-Deficient A. thaliana Mutants. Mol. Cell Proteomics **14**:1169-1182.

Navajas,R., Paradela,A. and Albar,J.P. (2011). Immobilized metal affinity chromatography/reversed-phase enrichment of phosphopeptides and analysis by CID/ETD tandem mass spectrometry. Methods Mol. Biol. **681**:337-348.

Ng,L.M., Soon,F.F., Zhou,X.E., West,G.M., Kovach,A., Suino-Powell,K.M., Chalmers,M.J., Li,J., Yong,E.L., Zhu,J.K., Griffin,P.R., Melcher,K. and Xu,H.E. (2011). Structural basis for basal activity and autoactivation of abscisic acid (ABA) signaling SnRK2 kinases. Proc. Natl. Acad. Sci. U. S. A **108**:21259-64

Nishimura,N., Yoshida,T., Kitahata,N., Asami,T., Shinozaki,K. and Hirayama,T. (2007). ABA-Hypersensitive Germination1 encodes a protein phosphatase 2C, an essential component of abscisic acid signaling in Arabidopsis seed. Plant J. **50**:935-949.

Nishimura,N., Sarkeshik,A., Nito,K., Park,S.Y., Wang,A., Carvalho,P.C., Lee,S., Caddell,D.F., Cutler,S.R., Chory,J., Yates,J.R. and Schroeder,J.I. (2010). PYR/PYL/RCAR family members are major in-vivo ABI1 protein phosphatase 2C-interacting proteins in Arabidopsis. Plant J. **61**:290-299.

Park,S.Y., Fung,P., Nishimura,N., Jensen,D.R., Fujii,H., Zhao,Y., Lumba,S., Santiago,J., Rodrigues,A., Chow,T.F.F., Alfred,S.E., Bonetta,D., Finkelstein,R., Provart,N.J.,

Desveaux,D., Rodriguez,P.L., McCourt,P., Zhu,J.K., Schroeder,J.I., Volkman,B.F. and Cutler,S.R. (2009). Abscisic Acid Inhibits Type 2C Protein Phosphatases via the PYR/PYL Family of START Proteins. Science **324**:1068-1071.

Pizzio,G.A., Rodriguez,L., Antoni,R., Gonzalez-Guzman,M., Yunta,C., Merilo,E., Kollist,H., Albert,A. and Rodriguez,P.L. (2013). The PYL4 A194T mutant uncovers a key role of PYR1-LIKE4/PROTEIN PHOSPHATASE 2CA interaction for abscisic acid signaling and plant drought resistance. Plant Physiol **163**:441-455.

Planes,M.D., Ninoles,R., Rubio,L., Bissoli,G., Bueso,E., Garcia-Sanchez,M.J., Alejandro,S., Gonzalez-Guzman,M., Hedrich,R., Rodriguez,P.L., Fernandez,J.A. and Serrano,R. (2015). A mechanism of growth inhibition by abscisic acid in germinating seeds of Arabidopsis thaliana based on inhibition of plasma membrane H+-ATPase and decreased cytosolic pH, K+, and anions. J. Exp. Bot. **66**:813-825.

Rodriguez,L., Gonzalez-Guzman,M., Diaz,M., Rodrigues,A., Izquierdo-Garcia,A.C., Peirats-Llobet,M., Fernandez,M.A., Antoni,R., Fernandez,D., Marquez,J.A., Mulet,J.M., Albert,A. and Rodriguez,P.L. (2014). C2-Domain Abscisic Acid-Related Proteins Mediate the Interaction of PYR/PYL/RCAR Abscisic Acid Receptors with the Plasma Membrane and Regulate Abscisic Acid Sensitivity in Arabidopsis. Plant Cell **26**:4802-4820.

Ryu,H., Cho,H., Bae,W. and Hwang,I. (2014). Control of early seedling development by BES1/TPL/HDA19-mediated epigenetic regulation of ABI3. Nat. Commun. **5**, 4138.

Saez,A., Apostolova,N., Gonzalez-Guzman,M., Gonzalez-Garcia,M.P., Nicolas,C., Lorenzo,O. and Rodriguez,P.L. (2004). Gain-of-function and loss-of-function phenotypes of the protein phosphatase 2C HAB1 reveal its role as a negative regulator of abscisic acid signalling. Plant J. **37**:354-369.

Saez,A., Rodrigues,A., Santiago,J., Rubio,S. and Rodriguez,P.L. (2008). HAB1-SWI3B interaction reveals a link between abscisic acid signaling and putative SWI/SNF chromatin-remodeling complexes in Arabidopsis. Plant Cell **20**:2972-2988.

Santiago,J., Rodrigues,A., Saez,A., Rubio,S., Antoni,R., Dupeux,F., Park,S.Y., Marquez,J.A., Cutler,S.R. and Rodriguez,P.L. (2009). Modulation of drought resistance by the abscisic acid receptor PYL5 through inhibition of clade A PP2Cs. Plant J. **60**:575-588.

Sen,P., Ghosh,S., Pugh,B.F. and Bartholomew,B. (2011). A new, highly conserved domain in Swi2/Snf2 is required for SWI/SNF remodeling. Nucleic Acids Res. **39**:9155-9166.

Sen,P., Vivas,P., Dechassa,M.L., Mooney,A.M., Poirier,M.G. and Bartholomew,B. (2013). The SnAC domain of SWI/SNF is a histone anchor required for remodeling. Mol. Cell Biol. **33**: 360-370.

Soon,F.F., Ng,L.M., Zhou,X.E., West,G.M., Kovach,A., Tan,M.H., Suino-Powell,K.M., He,Y., Xu,Y., Chalmers,M.J., Brunzelle,J.S., Zhang,H., Yang,H., Jiang,H., Li,J., Yong,E.L., Cutler,S., Zhu,J.K., Griffin,P.R., Melcher,K. and Xu,H.E. (2012). Molecular mimicry regulates ABA signaling by SnRK2 kinases and PP2C phosphatases. Science **335**:85-88.

Szerlong,H., Hinata,K., Viswanathan,R., Erdjument-Bromage,H., Tempst,P. and Cairns,B.R. (2008). The HSA domain binds nuclear actin-related proteins to regulate chromatin-remodeling ATPases. Nat. Struct. Mol. Biol. **15**:469-476.

Umezawa,T., Sugiyama,N., Mizoguchi,M., Hayashi,S., Myouga,F., Yamaguchi-Shinozaki,K., Ishihama,Y., Hirayama,T. and Shinozaki,K. (2009). Type 2C protein phosphatases directly regulate abscisic acid-activated protein kinases in Arabidopsis. Proc. Natl. Acad. Sci. U. S. A **106**:17588-17593

Umezawa,T., Sugiyama,N., Takahashi,F., Anderson,J.C., Ishihama,Y., Peck,S.C. and Shinozaki,K. (2013). Genetics and phosphoproteomics reveal a protein phosphorylation network in the abscisic acid signaling pathway in Arabidopsis thaliana. Sci. Signal. **6**:rs8.

Vlad,F., Rubio,S., Rodrigues,A., Sirichandra,C., Belin,C., Robert,N., Leung,J., Rodriguez,P.L., Lauriere,C. and Merlot,S. (2009). Protein phosphatases 2C regulate the activation of the Snf1-related kinase OST1 by abscisic acid in Arabidopsis. Plant Cell **21**: 3170-3184.

Vlad,F., Droillard,M.J., Valot,B., Khafif,M., Rodrigues,A., Brault,M., Zivy,M., Rodriguez,P.L., Merlot,S. and Lauriere,C. (2010). Phospho-site mapping, genetic and in planta activation studies reveal key aspects of the different phosphorylation mechanisms involved in activation of SnRK2s. Plant J. **63**:778-790.

Voinnet,O., Rivas,S., Mestre,P. and Baulcombe,D. (2003). An enhanced transient expression system in plants based on suppression of gene silencing by the p19 protein of tomato bushy stunt virus. Plant J. **33**:949-956.

Waadt,R., Schmidt,L.K., Lohse,M., Hashimoto,K., Bock,R. and Kudla,J. (2008). Multicolor bimolecular fluorescence complementation reveals simultaneous formation of alternative CBL/CIPK complexes in planta. Plant J. **56**:505-516.

Walter,M., Chaban,C., Schutze,K., Batistic,O., Weckermann,K., Nake,C., Blazevic,D., Grefen,C., Schumacher,K., Oecking,C., Harter,K. and Kudla,J. (2004). Visualization of protein interactions in living plant cells using bimolecular fluorescence complementation. Plant J. **40**:428-438.

Wang,P., Xue,L., Batelli,G., Lee,S., Hou,Y.J., Van Oosten,M.J., Zhang,H., Tao,W.A. and Zhu,J.K. (2013). Quantitative phosphoproteomics identifies SnRK2 protein kinase substrates and reveals the effectors of abscisic acid action. Proc. Natl. Acad. Sci. U. S. A **110**:11205-11210.

Weake,V.M. and Workman,J.L. (2010). Inducible gene expression: diverse regulatory mechanisms. Nat. Rev. Genet. **11**:426-437.

Wu,M.F., Sang,Y., Bezhani,S., Yamaguchi,N., Han,S.K., Li,Z., Su,Y., Slewinski,T.L. and Wagner,D. (2012). SWI2/SNF2 chromatin remodeling ATPases overcome polycomb repression and control floral organ identity with the LEAFY and SEPALLATA3 transcription factors. Proc. Natl. Acad. Sci. U. S. A **109**:3576-3581.

Wu,M.F., Yamaguchi,N., Xiao, J., Bargmann, B., Estelle, M., Sang, Y and Wagner, D. (2015). Auxin-regulated chromatin switch directs acquisition of flower primordium founder fate, eLife 2015;4:e09269.

Xue,L., Wang,P., Wang,L., Renzi,E., Radivojac,P., Tang,H., Arnold,R., Zhu,J.K. and Tao,W.A. (2013). Quantitative measurement of phosphoproteome response to osmotic stress in arabidopsis based on Library-Assisted eXtracted Ion Chromatogram (LAXIC). Mol. Cell Proteomics **12**:2354-2369.

Yaish,M.W., Colasanti,J. and Rothstein,S.J. (2011). The role of epigenetic processes in controlling flowering time in plants exposed to stress. J. Exp. Bot. **62**:3727-3735.

Yoo,S.D., Cho,Y.H. and Sheen,J. (2007). Arabidopsis mesophyll protoplasts: a versatile cell system for transient gene expression analysis. Nat. Protoc. **2**:1565-1572.

Yoshida,T., Mogami,J. and Yamaguchi-Shinozaki,K. (2015). Omics Approaches Toward Defining the Comprehensive Abscisic Acid Signaling Network in Plants. Plant Cell Physiol **56**:1043-1052.

Zhao,M., Yang,S., Liu,X. and Wu,K. (2015). Arabidopsis histone demethylases LDL1 and LDL2 control primary seed dormancy by regulating DELAY OF GERMINATION 1 and ABA signaling-related genes. Front Plant Sci. **6**:159.

Zhu,J., Jeong,J.C., Zhu,Y., Sokolchik,I., Miyazaki,S., Zhu,J.K., Hasegawa,P.M., Bohnert,H.J., Shi,H., Yun,D.J. and Bressan,R.A. (2008). Involvement of Arabidopsis HOS15 in histone deacetylation and cold tolerance. Proc. Natl. Acad. Sci. U. S. A **105**:4945-4950.

FIGURE LEGENDS

Figure 1. ABA-insensitivity is dependent on BRM activity in different genetic backgrounds. (A) Photographs of Columbia (Col-0) wild type, *brm-3*, *snrk2.2/2.3* and the *snrk2.2/2.3/brm-3* triple mutant grown for 7 d on MS medium either lacking or supplemented with the indicated ABA concentrations. Seeds were germinated in plates lacking or supplemented with ABA and after 7 d seedlings were rearranged on agar plates to illustrate seedling growth. Bars = 1cm. (B) Quantification of ABA-mediated inhibition of seedling establishment for the indicated genetic backgrounds. Approximately 100 seeds of each genotype were sown on each plate and scored for the presence of both green cotyledons and the first pair of true leaves 7 d later. Values are averages ± SE of three independent experiments. * indicates $P<0.05$ (Student's t test) compared to *snrk2.2/2.3* in the same assay conditions. (C) The root ABA-insensitive phenotype of *snrk2.2/2.3* is attenuated in *snrk2.2/2.3/brm-3*. Quantification of ABA-mediated root growth inhibition in the indicated genetic backgrounds. Data are averages ± SE from three independent experiments (n=30). * indicates $P<0.05$ (Student's t test) compared to *snrk2.2/2.3* in the same assay conditions. (D) The root ABA-insensitive phenotype of *HAB1* OE line is attenuated in *brm-101 HAB1* OE. Data are averages ± SE from three independent experiments (n=30, except *brm-101* with n=14). * indicates $P<0.05$ (Student's t test) compared to *HAB1* OE line in the same assay conditions.

Figure 2. BRM interacts with SnRK2.2/2.3/2.6 and HAB1/PP2CA clade A PP2Cs. (A) Domain architecture of the Arabidopsis BRM protein. (B, C, D) BiFC analyses show interaction between BRM and SnRK2s/PP2Cs. (B) Left: BiFC interaction of HAB1 and OST1/SnRK2.6 with BRM^N and BRM^C in the nucleus of *Arabidopsis* leaf protoplasts. The YFP fluorescence was merged with red fluorescence generated by chloroplasts. Right: Quantification of the percent YFP positive cells observed. Values are averages ± SE from three independent experiments. The number of protoplasts scored per interaction test was >600. NC: negative control. (C) Left: BiFC interaction of SnRK2.2, SnRK2.3 and

SnRK2.6 with BRM^N and BRM^C in the nucleus of tobacco leaf cells. Tobacco leaves were infiltrated with a mixture of Agrobacterium suspensions harbouring the indicated constructs and the silencing suppressor p19. Right: The BRM^N interaction was confirmed in Y2H assays. Dilutions (10^{-1}, 10^{-2} and 10^{-3}) of saturated cultures were spotted onto the plates, and photographs were taken after 5 days. Interaction was determined by growth assay on medium lacking His and Ade. Bars=20 μm. (D) Left: BiFC interaction of PP2CA and HAB1 with BRM^N and BRM^C. Right: Interaction was confirmed in Y2H assays conducted as in (C) except that growth in the case of HAB1 was also tested on –His + 0.1 mM 3AT medium. (E) coIP of BRM and SnRK2.2 or PP2CA. Double transgenic lines containing ProBRM:BRM-GFP and HA-tagged SnRK2.2 or PP2CA were used for coIP experiments. Nuclear soluble protein extracts prepared from mock- or ABA-treated plants (50 μM for 1h) were immunoprecipitated using either α-HA (left) or α-GFP (right). CoIP was revealed using α-GFP or α-HA, respectively. Histograms show the quantification of the protein signal obtained with analyzer LAS3000 and Image Guache V4.0 software.

Figure 3. Phosphorylation of the carboxy-terminal domain of BRM by OST1 is reversed by PP2CA. (A) In vitro phosphorylation of BRM C2 and BRM C3 fragments by OST1/SnRK2.6. Subsequent addition of PP2CA dephosphorylates BRM C2 and BRM C3, whereas co-incubation of PP2CA with PYL8 in the presence of ABA (10 μM) prevents the dephosphorylation of BRM C2 and BRM C3. The BRM D2 fragment is not phosphorylated by OST1, in contrast to a positive control (ABF2 ΔC; Pizzio et al., 2013) or the BRM C3 fragment. (B) Identification of four phosphorylation sites in BRM C-terminal region. Spectra obtained by tandem mass spectrometry of phosphorylated peptides are shown and annotated. CID and ETD spectra obtained by LC–MS/MS system were searched against the SwissProt database using a licensed version v.2.3.02 of Mascot (Matrix Science, London, UK) as search engine. The location of the four phosphorylation sites in the C-terminal part of BRM is indicated by violet symbols. The fragmentation pattern of two phosphorylated peptides in the CID/ETD spectra did not allow the unambiguous assignment of the phosphate group to specific S/T residues (in brackets)

Figure 4. Enhanced ABA sensitivity of a BRM$^{S1760D\ S1762D}$ phosphomimetic mutant compared to wt. (A) PYL ABA receptors block the interaction of PP2CA with BRM in an ABA-dependent manner. Reconstitution of the ABA sensing/signaling pathway in yeast revealed that ABA receptors PYL4 and PYL5 block the interaction between BRM^{N} and PP2CA upon signal perception. (B) Presence of PP2CA does not interfere with the interaction between SnRK2.3 and BRM^{N} in yeast. (C) The BRM phosphomimetic mutant (2S-D) shows ABA-hypersensitivity during seedling establishment compared to wt, *brm-3, or brm-1* mutant transformed with wild-type BRM (2S). Left: photographs of the indicated genetic backgrounds grown for 4 d on MS medium either lacking or supplemented with ABA. Bar=0.5 cm. Right: quantification of cotyledon greening 4 days after sowing. Values are averages of two independent biological experiments. The error bars are proportional to the standard error of the pooled percentage computed using binominal distribution. * indicates P<0.01 (Chi square test) compared to wt in the same assay conditions. (D) BRM$^{S1760A\ S1762A}$ phosphomutant does not show ABA hypersensitivity during seedling establishment compared to wt. (E) Expression of *ABI5*, a direct BRM target, during seedling establishment in BRM phosphomimetic mutant compared to wt and *brm-3.* (F) A model for the regulation of BRM activity through inhibitory SnRK2-dependent phosphorylation and restorative PP2C-dependent dephosphorylation. When ABA levels increase, SnRK2s are activated and clade A PP2Cs inhibited by PYR/PYL ABA receptors. This allows SnRK2s to phosphorylate BRM, which leads to inhibition of BRM activity and *ABI5* induction. At low ABA levels, dephosphorylation of BRM by PP2CA/HAB1 restores BRM activity and repression of *ABI5* expression.

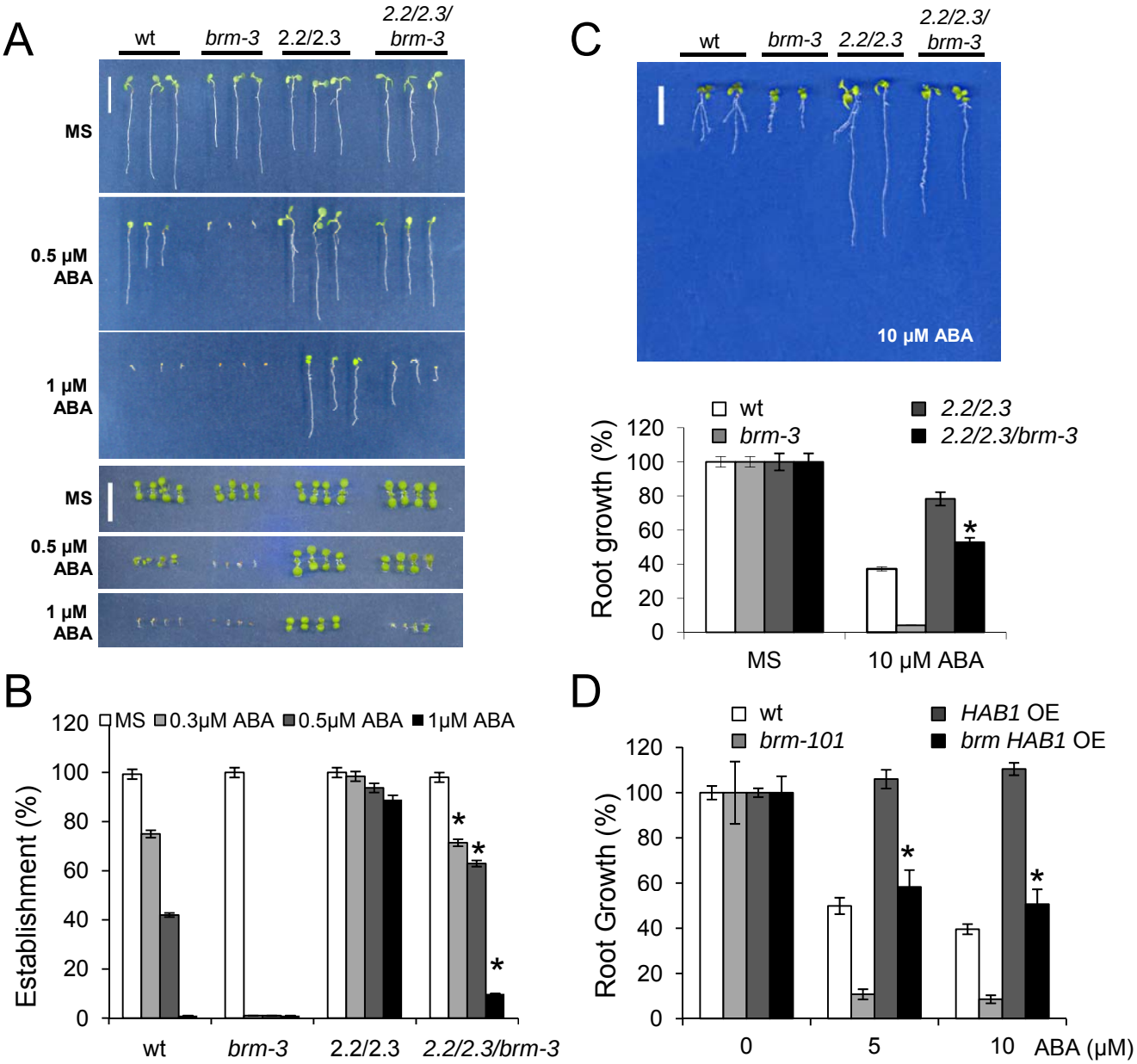

Figure 1. ABA-insensitivity is dependent on BRM activity in different genetic backgrounds. (A) Photographs of Columbia (Col-0) wild-type, *brm-3*, *snrk2.2/2.3* and the *snrk2.2/2.3/brm-3* triple mutant grown for 7 d on MS medium either lacking or supplemented with the indicated ABA concentrations. Seeds were germinated in plates lacking or supplemented with ABA and after 7 d seedlings were rearranged on agar plates to illustrate seedling growth. Bars = 1cm. (B) Quantification of ABA-mediated inhibition of seedling establishment for the indicated genetic backgrounds. Approximately 100 seeds of each genotype were sown on each plate and scored for the presence of both green cotyledons and the first pair of true leaves 7 d later. Values are averages ± SE of three independent experiments. * indicates P<0.05 (Student's t test) compared to *snrk2.2/2.3* in the same assay conditions. (C) The root ABA-insensitive phenotype of *snrk2.2/2.3* is attenuated in *snrk2.2/2.3/brm-3*. Quantification of ABA-mediated root growth inhibition in the indicated genetic backgrounds. Data are averages± SE from three independent experiments (n=30). * indicates P<0.05 (Student's t test) compared to *snrk2.2/2.3* in the same assay conditions. (D) The root ABA-insensitive phenotype of *HAB1* OE line is attenuated in *brm-101 HAB1* OE. Data are averages± SE from three independent experiments (n=30, except *brm-101* with n=14). * indicates P<0.05 (Student's t test) compared to *HAB1* OE line in the same assay conditions.

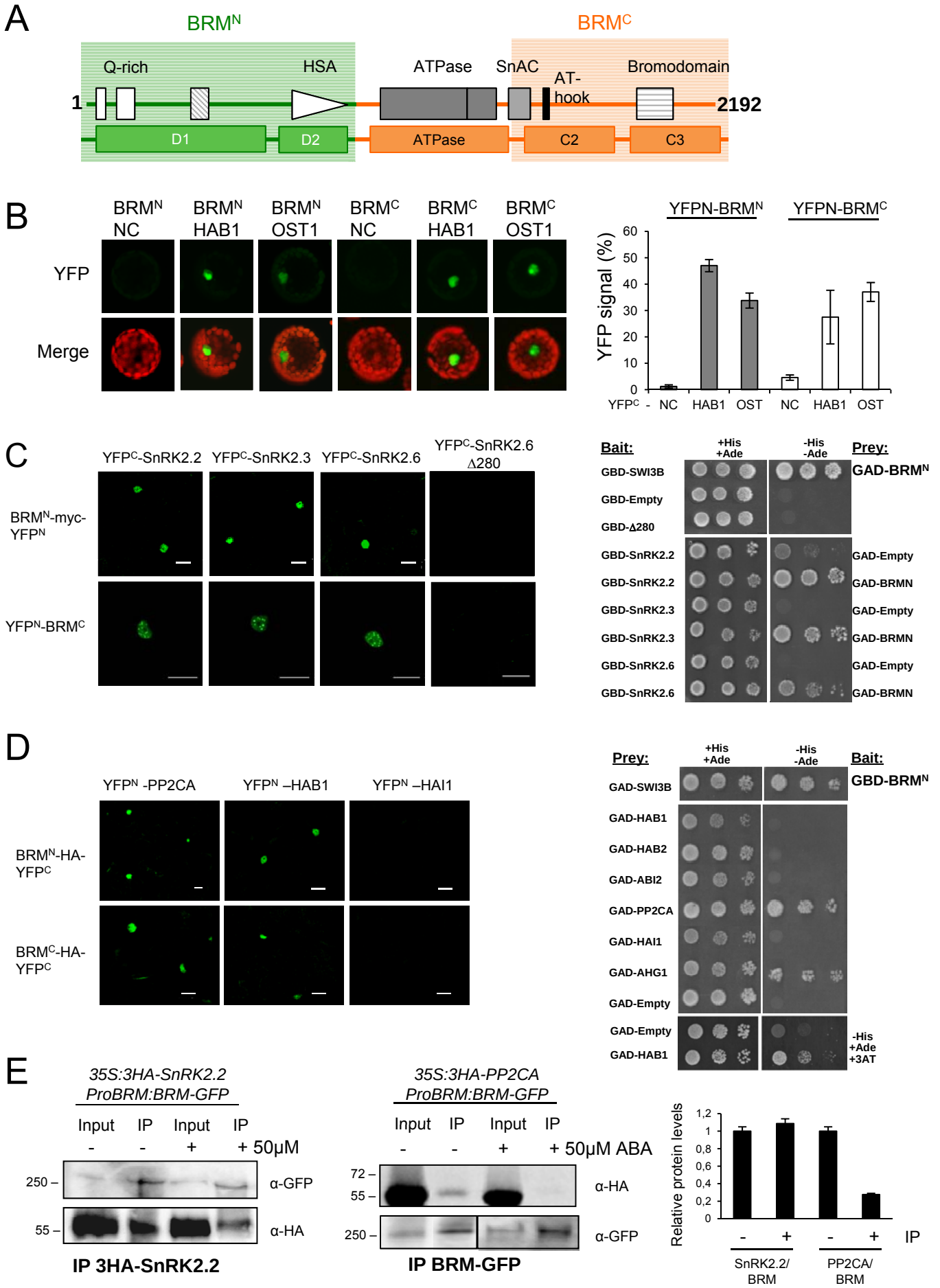
A
BRMN
BRMC
Q-rich
HSA
ATPase
SnAC
AT-hook
Bromodomain
1
2192
D1
D2
ATPase
C2
C3
B
BRMN NC
BRMN HAB1
BRMN OST1
BRMC NC
BRMC HAB1
BRMC OST1
YFP
Merge
YFPN-BRMN
YFPN-BRMC
YFP signal (%)
60
50
40
30
20
10
0
YFPC - NC HAB1 OST NC HAB1 OST
C
YFPC-SnRK2.2
YFPC-SnRK2.3
YFPC-SnRK2.6
YFPC-SnRK2.6 Δ280
BRMN-myc-YFPN
YFPN-BRMC
Bait:
+His +Ade
-His -Ade
Prey:
GBD-SWI3B
GBD-Empty
GBD-Δ280
GBD-SnRK2.2
GBD-SnRK2.2
GBD-SnRK2.3
GBD-SnRK2.3
GBD-SnRK2.6
GBD-SnRK2.6
GAD-BRMN
GAD-Empty
GAD-BRMN
GAD-Empty
GAD-BRMN
GAD-Empty
GAD-BRMN
D
YFPN -PP2CA
YFPN –HAB1
YFPN –HAI1
BRMN-HA-YFPC
BRMC-HA-YFPC
Prey:
+His +Ade
-His -Ade
Bait:
GAD-SWI3B
GAD-HAB1
GAD-HAB2
GAD-ABI2
GAD-PP2CA
GAD-HAI1
GAD-AHG1
GAD-Empty
GAD-Empty
GAD-HAB1
GBD-BRMN
-His +Ade +3AT
E
35S:3HA-SnRK2.2
ProBRM:BRM-GFP
Input IP Input IP
- - + + 50μM
250 –
55 –
α-GFP
α-HA
IP 3HA-SnRK2.2
35S:3HA-PP2CA
ProBRM:BRM-GFP
Input IP Input IP
- - + + 50μM ABA
72 –
55 –
250 –
α-HA
α-GFP
IP BRM-GFP
Relative protein levels
1,2
1
0,8
0,6
0,4
0,2
0
- + - + IP
SnRK2.2/ BRM
PP2CA/ BRM

Figure 2. BRM interacts with SnRK2.2/2.3/2.6 and HAB1/PP2CA clade A PP2Cs. (A) Domain architecture of the Arabidopsis BRM protein. (B, C, D) BiFC analyses show interaction between BRM and SnRK2s/PP2Cs. (B) Left: BiFC interaction of HAB1 and OST1/SnRK2.6 with BRM^N and BRM^C in the nucleus of *Arabidopsis* leaf protoplasts. The YFP fluorescence was merged with red fluorescence generated by chloroplasts. Right: Quantification of the percent YFP positive cells observed. Values are averages± SE from three independent experiments. The number of protoplasts scored per interaction test was >600. (C) Left: BiFC interaction of SnRK2.2, SnRK2.3 and SnRK2.6 with BRM^N and BRM^C in the nucleus of tobacco leaf cells. Tobacco leaves were infiltrated with a mixture of Agrobacterium suspensions harbouring the indicated constructs and the silencing suppressor p19. Bar corresponds to 20 µm. Right: The BRM^N interaction was confirmed in Y2H assays. Dilutions (10^{-1}, 10^{-2} and 10^{-3}) of saturated cultures were spotted onto the plates, and photographs were taken after 5 days. Interaction was determined by growth assay on medium lacking His and Ade. Bars=20 µm (D) Left: BiFC interaction of PP2CA and HAB1 with BRM^N and BRM^C. Bar corresponds to 20 µm. Right: Interaction was confirmed in Y2H assays conducted as in (C) except that growth in the case of HAB1 was also tested on –His + 0.1 mM 3AT medium. (E) coIP of BRM and SnRK2.2 or PP2CA. Double transgenic lines containing ProBRM:BRM-GFP and HA-tagged SnRK2.2 or PP2CA were used for coIP experiments. Nuclear soluble protein extracts prepared from mock- or ABA-treated plants (50 µM for 1h) were immunoprecipitated using either a-HA (left) or a-GFP (right). CoIP was revealed using a-GFP or a-HA, respectively. Histograms show the quantification of the protein signal obtained with analyzer LAS3000 and Image Guache V4.0 software.

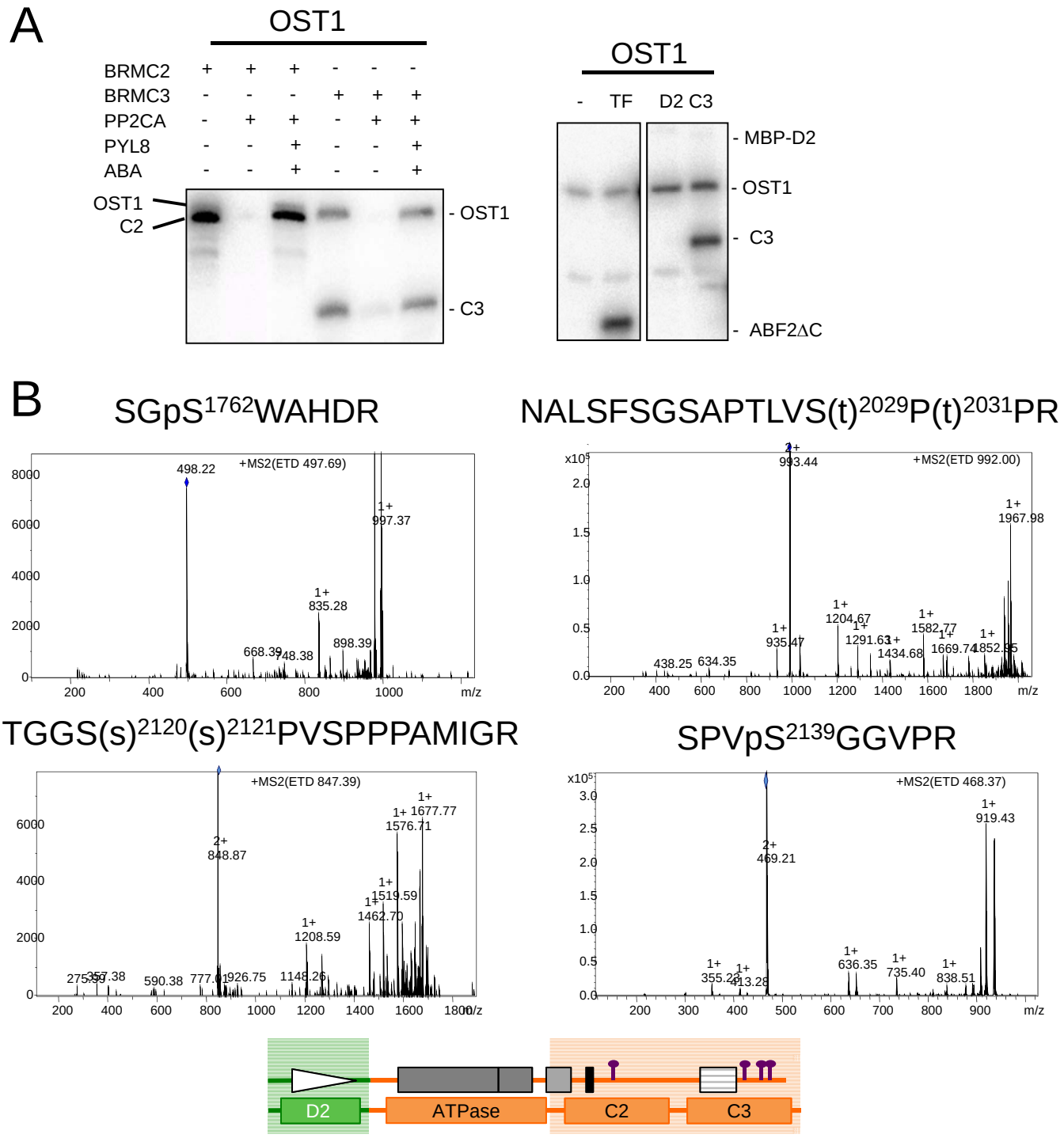

Figure 3. Phosphorylation of the carboxy-terminal part of BRM by OST1 is reversed by PP2CA. (A) In vitro phosphorylation of BRM C2 and BRM C3 fragments by OST1/SnRK2.6. Subsequent addition of PP2CA dephosphorylates BRM C2 and BRM C3, whereas co-incubation of PP2CA with PYL8 in the presence of ABA (10 uM) prevents the dephosphorylation of BRM C2 and BRM C3. The BRM D2 fragment is not phosphorylated by OST1, in contrast to ABF2 DC or BRM C3 fragments. (B) Identification of four phosphorylation sites in BRM C-terminal region. Spectra obtained by tandem mass spectrometry of phosphorylated peptides are shown and annotated. CID and ETD spectra obtained by LC–MS/MS system were searched against the SwissProt database using a licensed version v.2.3.02 of Mascot (Matrix Science, London, UK) as search engine. Localization of the four phosphorylation sites in the C-terminal part of BRM (violet symbols). The fragmentation pattern of two phosphorylated peptides in the CID/ETD spectra did not allow the unambiguous assignment of the phosphate group to specific S/T residues (in brackets)

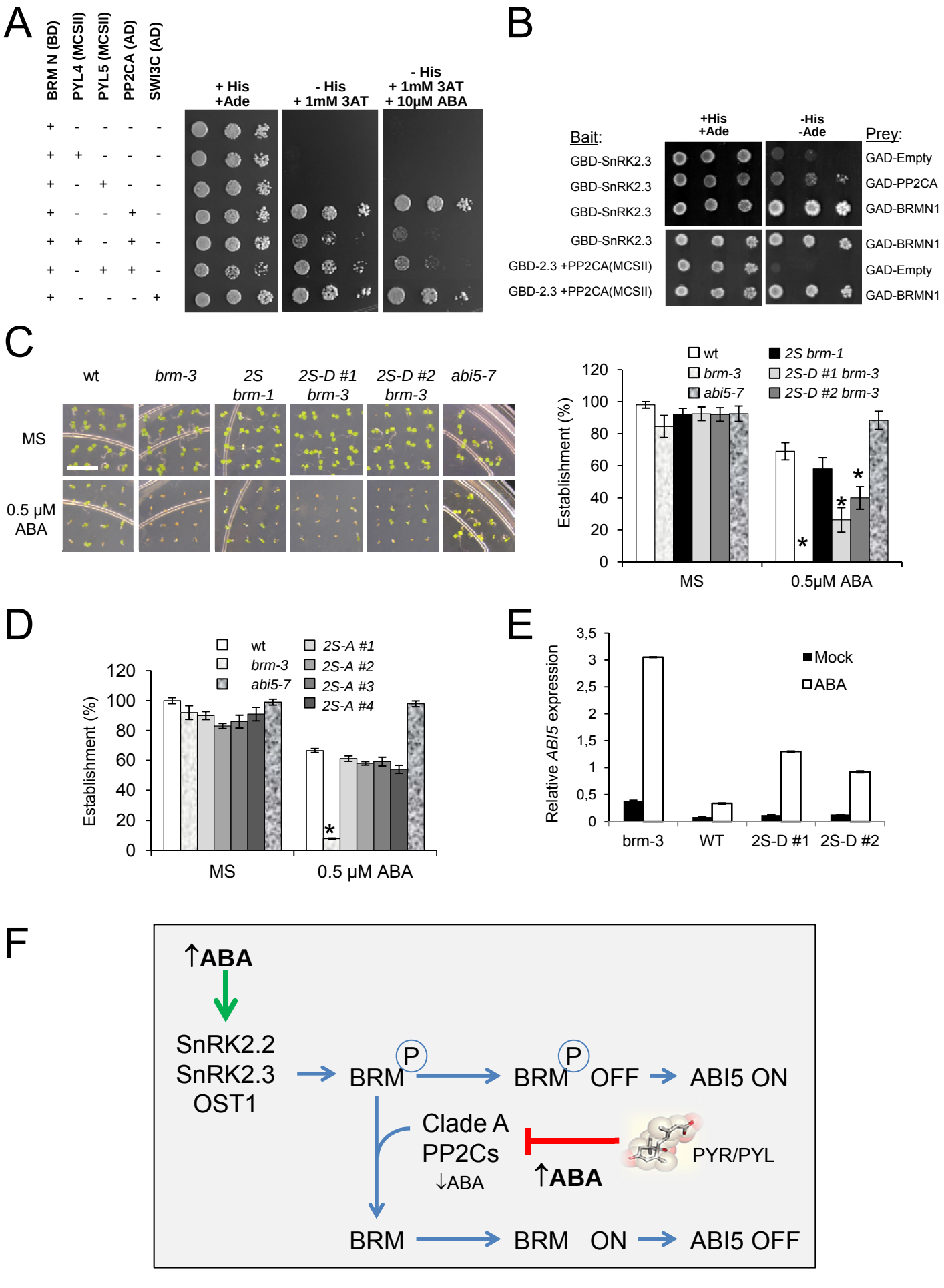
A
BRM N (BD)
PYL4 (MCSII)
PYL5 (MCSII)
PP2CA (AD)
SWI3C (AD)
+ His +Ade
- His + 1mM 3AT
- His + 1mM 3AT + 10µM ABA
B
Bait:
Prey:
+His +Ade
-His -Ade
GBD-SnRK2.3
GAD-Empty
GAD-PP2CA
GAD-BRMN1
GBD-2.3 +PP2CA(MCSII)
C
wt
brm-3
2S brm-1
2S-D #1 brm-3
2S-D #2 brm-3
abi5-7
MS
0.5 µM ABA
Establishment (%)
0.5µM ABA
D
2S-A #1
2S-A #2
2S-A #3
2S-A #4
0.5 µM ABA
E
Relative ABI5 expression
Mock
ABA
brm-3
WT
2S-D #1
2S-D #2
F
↑ABA
SnRK2.2
SnRK2.3
OST1
BRM
P
BRM OFF
ABI5 ON
Clade A
PP2Cs
↓ABA
↑ABA
PYR/PYL
BRM ON
ABI5 OFF

Figure 4. Enhanced ABA sensitivity of a $BRM^{S1760D\ S1762D}$ phosphomimetic mutant compared to wt. (A) PYL ABA receptors block the interaction of PP2CA with BRM in an ABA-dependent manner. Reconstitution of the ABA sensing/signaling pathway in yeast revealed that ABA receptors PYL4 and PYL5 block the interaction between BRM^{N} and PP2CA upon signal perception. (B) Presence of PP2CA does not interfere with the interaction between SnRK2.3 and BRM^{N} in yeast. (C) The BRM phosphomimetic mutant (2S-D) shows ABA-hypersensitivity during seedling establishment compared to wt, *brm-3, or brm-1* mutant transformed with wild-type BRM (2S). Left: photographs of the indicated genetic backgrounds grown for 4 d on MS medium either lacking or supplemented with ABA. Bar=0.5 cm. Right: quantification of cotyledon greening 4 days after sowing. Values are averages of two independent biological experiments. The error bars are proportional to the standard error of the pooled percentage computed using binominal distribution. * indicates $P<0.01$ (Chi square test) compared to wt in the same assay conditions. (D) $BRM^{S1760A\ S1762A}$ phosphomutant does not show ABA hypersensitivity during seedling establishment compared to wt. (E) Expression of *ABI5*, a direct BRM target, during seedling establishment in BRM phosphomimetic mutant compared to wt and *brm-3.* (F) A model for the regulation of BRM activity through inhibitory SnRK2-dependent phosphorylation and restorative PP2C-dependent dephosphorylation. When ABA levels increase, SnRK2s are activated and clade A PP2Cs inhibited by PYR/PYL ABA receptors. This allows SnRK2s to phosphorylate BRM, which leads to inhibition of BRM activity and *ABI5* induction. At low ABA levels, dephosphorylation of BRM by PP2CA/HAB1 restores BRM activity and repression of *ABI5* expression.

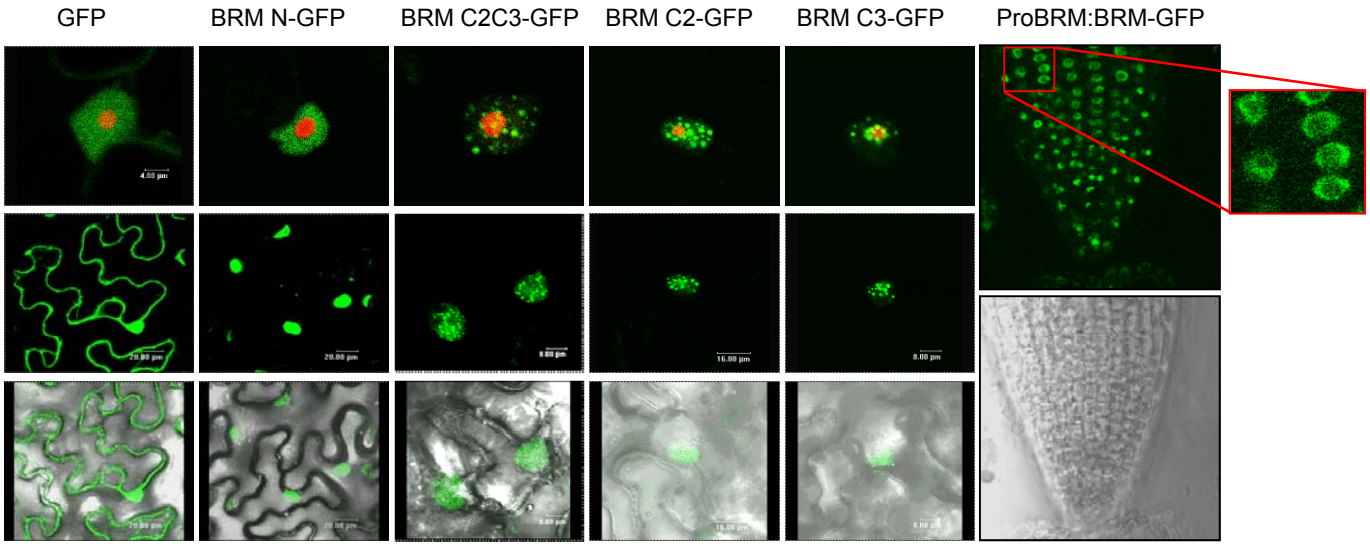

Supplemental Figure 1. BRM fragments are localized in the nucleus of *Agrobacterium*-infiltrated tobacco leaves. Confocal microscopy of transiently transformed *N. benthamiana* epidermal cells co-expressing green fluorescent protein (GFP) or GFP-BRM fusions and the nucleolar marker Fibrilarin tagged with red fluorescent protein (RFP). Location in nuclear speckles was observed for BRM C2-GFP and BRM C3-GFP, whereas BRM N-GFP showed a diffuse nuclear pattern as nuclear GFP. Bars correspond to 20 μM. Right panel show CSLM of roots from transgenic lines expressing full-length BRM-GFP

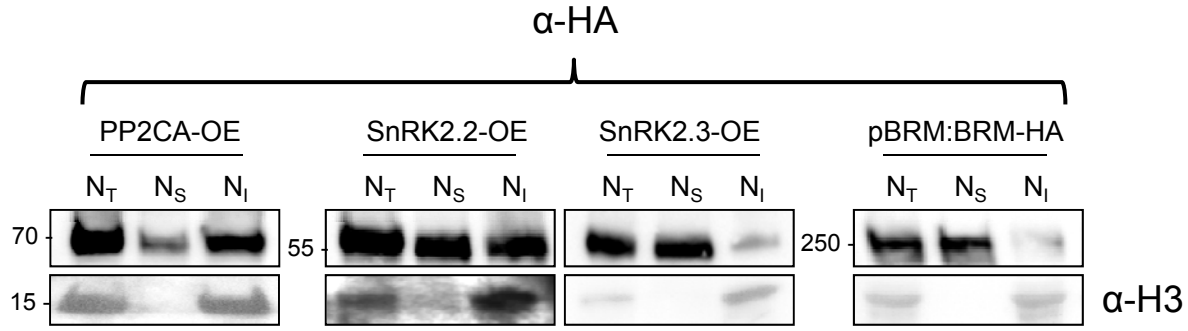

Supplemental Figure 2. Biochemical fractionation and immunoblot analysis of protein extracts prepared from *Arabidopsis* transgenic plants expressing 35:3HA-PP2CA, 35:3HA-SnRK2.2, 35:3HA-SnRK2.3, and ProBRM:BRM–HA. Nuclear total (Nt), nuclear soluble (Ns) and nuclear insoluble (Ni) protein extracts were analyzed by immunoblotting using α-HA and α-H3 antibodies

Supplemental Figure 3. BRM phosphopheptides in PhosPhAt 4.0 identified through *in vivo* phosphoproteomic studies and *in vitro* OST1 phosphorylation assays of BRM C2 and BRM C3 fragments (this work).

green, phosphopeptides N-terminal located
blue and red, phosphopeptides C-terminal located
red, phosphorylation sites identified in this work after in vitro OST1 phosphorylation

M[1]QSGGSGGGPARNPAMGPAGRTASTSSAASPSSSSSSVQQQQQQQQQQQQQQQLASRQQQQQHRN
SDTNENMFAYQPGGVQGMMGGGNFASSPGSMQMPQQSRNFFESPQQQQQQQQQGSSTQEGQQNFN
PMQQAYIQFAMQAQHQKAQQQARMGMVGSSSVGKDQDARMGMLNMQDLNPSSQPQASSSKPSGDQ
FARGERQTESSSQQRNETKSHPQQQVGTGQLMPGNMIRPMQAPQAQQLVNNMGNNQLAFAQQWQA
MQAWARERNIDLSHPANASQMAHILQARMAAQQKAGEGNVASQSPSIPISSQPASSSVVPGENSP
HANSASDISGQSGSAKARHALSTGSFApSTSSPRMVNPAMNPFSGQGRENPMYPRHLVQPTNGMP
SGNPLQTSANETPVLDQNASTKKSLGPAEHLQMQQPRQLNTPTPNLVAPSDTGPLSNSSLQSGQG
TQQAQQRSGFTKQQLHVLKAQILAFRRLKKGEGSLPPELLQAISPPPLELQTQRQIpSPAIGKVQ
DRSSDKTGEDQARSLECGKESQAAApSSNGPIFSKEEDNVGDTEVALTTGHSQLFQNLGKEAT(S
)TDVATKEEQQTDVFPVKSDQGADSSTQKNPRSDSTADKGKAVASDG(S)QSKVPPQANpSPQPP
KDTASARKYYGPLFDFPFFTRKLDSYGSATANANNNLTLAYDIKDLICEEGAEFLSKKRTDSLKK
INGLLAKNLERKRIRPDLVLRLQIEEKKLRLSDLQSRVREEVDRQQQEIMSMPDRPYRKFVRLCE
RQRLEMNRQVLANQKAVREKQLKTIFQWRKKLLEAHWAIRDARTARNRGVAKYHEKMLREFSKRK
DDGRNKRMEALKNNDVERYREMLLEQQTNMPGDAAERYAVLSSFLTQTEDYLHKLGGKITATKNQ
QEVEEAANAAAVAARLQGLSEEEVRAAATCAREEVVIRNRFTEMNAPKENSSVNKYYTLAHAVNE
VVVRQPSMLQAGTLRDYQLVGLQWMLSLYNNKLNGILADEMGLGKTVQVMALIAYLMEFKGNYGP
HLIIVPNAVLVNWKSELHTWLPSVSCIYYVGTKDQRSKLFSQEVCAMKFNVLVTTYEFIMYDRSK
LSKVDWKYIIIDEAQRMKDRESVLARDLDRYRCQRRLLLTGTPLQNDLKELWSLLNLLLPDVFDN
RKAFHDWFAQPFQKEGPAHNIEDDWLETEKKVIVIHRLHQILEPFMLRRRVEDVEGSLPAKVSVV
LRCRMSAIQSAVYDWIKATGTLRVDPDDEKLRAQKNPIYQAKIYRTLNNRCMELRKACNHPLLNY
PYFNDFSKDFLVRSCGKLWILDRILIKLQRTGHRVLLFSTMTKLLDILEEYLQWRRLVYRRIDGT
TSLEDRESAIVDFNDPDTDCFIFLLSIRAAGRGLNLQTADTVVIYDPDPNPKNEEQAVARAHRIG
QTREVKVIYMEAVVEKLSSHQKEDELRSGGpS[1452]VDLEDDMAGKDRYIGSIEGLIRNNIQQYKID
MADEVINAGRFDQRTTHEERRMTLETLLHDEERYQETVHDVPSLHEVNRMIARSEEEVELFDQMD
EEFDWTEEMTNHEQVPKWLRASTREVNATVADLSKKPSKNMLSSpS[1593]NLIVQPGGPGGERKRGR
PKSKKINYKEIEDDIAGYpS[1629]EEpS[1632]pS[1633]EERNIDpS[1640]NEEEGDIRQFDDDELpT[1657]GA
LGDHQTNKGEFDGENPVCGYDYPPGSGSYKKNPPRDDAGSSGSSPE(S)HRSKEMApS[1714]PVpS[17
18]pS[1719]QKFGpS[1723]LSALDTRPGpS[1733]VSKRLLDDLEEGEIAASGDSHIDLQRpS[1760]GpS[1762]WA
HDRDEGDEEQVLQPTIKRKRSIRLRPRQTAERVDGSEMPAAQPLQVDRSYRSKLRTVVDSHSSRQ
DQSDSSSRLRSVPAKKVASTSKLHVSSPKSGRLNATQLTVEDNAEASRE(T)WDGpT[1883]pS[1884]P
IpS[1887](S)(S)NAGARMSHIIQKRCKIVISKLQRRIDKEGQQIVPMLTNLWKRIQNGYAAGGVNN
LLELREIDHRVERLEYAGVMELASDVQLMLRGAMQFYGFSHEVRSEAKKVHNLFFDLLKMSFPDT
DFREARNALSFSGSAPTLVpS[2028]pT[2029]PTPRGAGISQGKRQKLVNEPEpT[2051]EPpS[2054]pS[2055]P
QR(s)QQRENSRIRVQIPQKETKLGGTTSHTDESPILAHPGELVICKKKRKDREKSGPKTRpT[2116]
GGSpS[2120]pS[2121]PVpS[2124]PPPAMIGRGLRpS[2136]PVpS[2139]GGVPRETRLAQQQRWPNQPTHPNNS
GAAGDSVGWANPVKRLRTDSGKRRPSHL[2192]

Supplemental Figure 4. Residues S1760 and S1762 of Arabidopsis thaliana BRM are evolutionary conserved in different plant species. *Medicago truncatula, Glycine max, Populus trichocarpa, Ricinus communis, Vitis vinifera, Solanum lycopersicum, Zea mays, Sorghum bicolor, Oryza sativa*

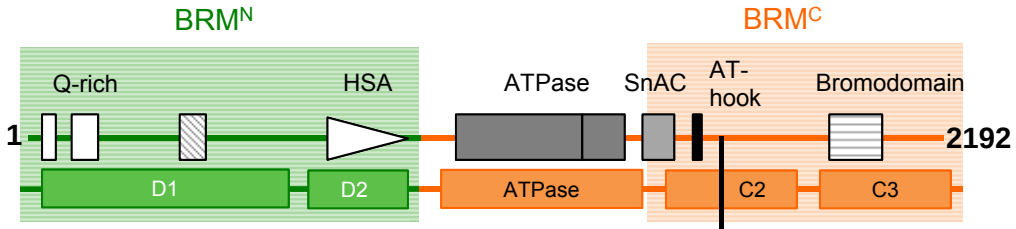


```
M. truncatula     Q-KFGSLSALDARPGSISK-KNDELEEGEIAVSFDSHMEHQQSGSWIHDRDEGEDEQVLQ 1749
G. max            Q-KFGSLSALDARPSSISKRMTDELEEGEIAVSGDSHMDHQQSGSWIHDRDEGEDEQVLQ 1802
P. trichocarpa    Q-KFGSLSALDARPGSLPKKLPDELEEGEIAVSGDSHVDHQQSGSWMHDRDEGEDEQVLQ 1805
R. communis       Q-KFGSLSALDARPGSISKKLPDELEEGEIAVSGDSHLDHQQSGSWIHDREEGEDEQVLQ 1807
V. vinefera       R-KFGSLSALDARPSSLSKRLPDELEEGEIAVSGDSHMDHQQSGSWIHDRDEGEDEQVLQ 1818
A. thaliana       Q-KFGSLSALDTRPGSVSKRLLDDLEEGEIAASGDSHIDLQRSGSWAHDRDEGDEEQVLQ 1777
S. lycopersicum   QQKFGSLSALDARPSSRAKRMADELEEGEIAVSGDSHVDLQQSGSWIQDRDEGEDEQVLQ 1803
Z. mays           SKKLRSLSALDARPGTLSKRTPDDLEEGEIAMSGDSHMDLQQSGSWNHERDDGEDEQVLQ 1756
S. bicolor        SKKLRSLSALDARPVSSSKRTPDDLEEGEIAMSGDSHMDLQQSGSWNHERDDGEDEQVLQ 1701
O. sativa         SKKLRSLSALDSRPGALSKRTADDLEEGEIALSGDSHLDLQQSGSWNHERDDGEDEQVVQ 1758
                    *: ******:** : .*   *:******* * ***:: *:**** ::*::*::***:*
```

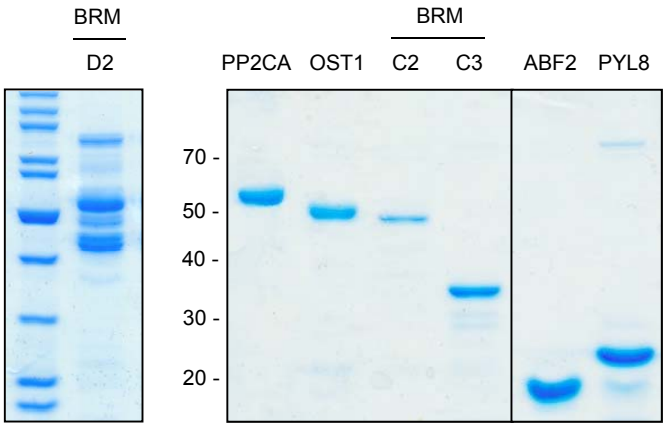

Supplemental Figure 5. Coomassie gel staining of the proteins used in the phosphorylation assay. MBP-BRM D2 was purified using amylose affinity chromatography (left panel), whereas His-tagged PP2CA, OST1, BRM C2, BRM C3, ABF2ΔC and PYL8 were purified using Ni-NTA affinity chromatography